2013

Biomarker and Sedimentological Investigations of MIS 8 through MIS 12 from Lake El'gygytgyn, NE Arctic Russia

Jeremy H. Wei
jeremyhcwei@gmail.com

BIOMARKER AND SEDIMENTOLOGICAL INVESTIGATIONS OF MIS 8 THROUGH MIS 12 FROM LAKE EL'GYGYTGYN, NE ARCTIC RUSSIA

A Thesis Presented

By

JEREMY H. WEI

Submitted to the Graduate School of the
University of Massachusetts – Amherst in partial fulfillment
of the requirements for the degree of

MASTER OF SCIENCE

September 2013

Geosciences

BIOMARKER AND SEDIMENTOLOGICAL INVESTIGATIONS OF MIS 8 THROUGH MIS 12 FROM LAKE EL'GYGYTGYN, NE ARCTIC RUSSIA

A Thesis Presented

By

JEREMY H. WEI

Approved as to style and content by:

_____

Julie Brigham-Grette, Chair

_____

David Finkelstein, Member

_____

Isla Castaneda, Member

_____

R. Mark Leckie, Department Head
Geosciences

ABSTRACT

BIOMARKER AND SEDIMENTOLOGICAL INVESTIGATIONS OF MIS 8 THROUGH MIS 12 FROM LAKE EL'GYGYTGYN, NE ARCTIC RUSSIA

SEPTEMBER 2013

JEREMY WEI, B.S., TUFTS UNIVERSITY

M.S., UNIVERSITY OF MASSACHUSETTS AMHERST

Directed by: Professor Julie Brigham-Grette

Multiple proxy analysis of lake sediment records are crucial for understanding changes in environmental and climate conditions over historical and geological time. Most recently, the use of biomarker proxies coupled with sedimentological investigations provides a new approach for gaining insight into the lake processes that capture information about past climate change. This approach is applied here to better understand the paleoclimate record from Lake El'gygytgyn in Western Beringia. Multiple organic geochemical compound concentrations were measure as proxies for both aquatic and terrestrial biological productivity. Measurements of *n*-alkane (plant leaf waxes) as well as concentrations of the compounds arborinol (marker for trees), dinosterol (dinoflagellates), and long chain (C_{28} – C_{32}) 1,15 *n*-alkyl diols (eustigmatophyte algae) demonstrate warming conditions around Lake El'gygytgyn during MIS 9 and MIS 11, especially when compared to diatom production and palynological investigations from Melles et al. (2012). These time periods illustrate the presence of extensive forest cover as well as elevated concentrations of all aquatic biomarkers analyzed, corroborating their "super interglacial" designation. Analysis of branched glycerol dialkyl glycerol tetraethers, a relatively new proxy used to estimate mean annual temperatures and soil pH, was applied also suggesting warming conditions during MIS 9 and MIS 11, although further calibration techniques are needed to accurately estimate temperature changes.

Sedimentological results include the analysis of bulk mineralogy, clay mineralogy, iron oxide, and color measurements for the same MIS 8 through MIS 12 interval. The hue color parameter, measured from high resolution core scans, suggests a link to global climate records, with green sediments reflective of cold intervals and red sediments indicative of warmer climate conditions. Validation of the color record was done in part by analyzing the clay mineralogy and the abundances of clay minerals. These data show that clay deposition dominates interglacial periods. Moreover the clay polytypes can be linked to bedrock weathering. Bulk mineralogy measurements allow for the reconstruction of synthetic color spectra which link mineralogy to sediment color. Overprinted on the mineralogical color signal is red color staining from iron oxide minerals, formed within the catchment during wet intervals when increasing amounts of eroded Fe – bearing silicate minerals are available for oxidation. If true, interpretation of the hue record then suggests hue is a proxy for wet/dry conditions within the lake, and when paired with the biomarker analysis shows significant warmer and wetter conditions during MIS 9 and 11. However, the hue record also demonstrates notable variability outside of these two interglacial periods, not recognized by other proxies, are not currently well understood. Overall, the multi-proxy results from this work can be further applied to the longer temporal scale of the Lake El'gygytgyn sediment core, and potentially elucidate climate changes deeper into the Pleistocene, and even into the Pliocene portions of the sediment record.

TABLE OF CONTENTS

LIST OF TABLES

LIST OF FIGURES

Figure Page

CHAPTER 1

INTRODUCTION

The study of paleoclimatology aids in the understanding of past changes, and these changes provide the much needed context for assessing the impact of current anthropogenic climate change. Paleoclimate investigations from sensitive areas of the planet in particular provide crucial information concerning the magnitude and intensity of potential future changes. Although the sensitivity of Arctic regions to changing climate conditions is demonstrated by rapidly diminishing summer sea ice (Serreze et al., 2007; Maslanik et al., 2007), investigations of past interglacial records from the Arctic beyond the last interglacial terrestrial environment are few. Lake El'gygytgyn, located in the the Far East Russian Arctic (6°30 N, 172°50 E), was drilled in 2009, yielding the longest lacustrine record from the Arctic, providing an unprecedented record of past Arctic Climate change. Formed by an impact event at 3.58 Ma (Layer, 2000), the lake catchment escaped past glaciations largely due to the regionally cold and dry climate (Glushkova, 1999; Nolan et al., 2012), preventing the growth of large ice sheets. Furthermore, it is located in a region where little is known about the interactions between the large Russian Arctic and climate dynamics. Specifically, past paleoclimate studies at the lake have shed new light on the lake's sensitivity to periods of global warmth and cooling, known as interglacial/glacial cycles. The 2009 drilling campaign, conducted as part of the Continental Drilling Program (ICDP – site 5011), yielded sediment cores dating back to the 3.6 Ma within the Pliocene epoch, comprising the longest continuous terrestrial climate record from the Arctic. Studies of Lake El'gygytgyn sediments is now producing critical new data that informs us of the role of the Arctic in global and regional change.

The fidelity and continuity of the lake El'gygytgyn record offers an unprecedented opportunity to better understand the character and intensity of past interglacials. Interglacial and glacial time periods have fluctuated in length and magnitude since the inception of Northern Hemisphere ice sheets ca 2.7 ma (Brigham-Grette et al., 2013), and time periods demonstrating elevated levels of warmth are of particular interest as possible analogs for the future. The interglacial period known as Marine Isotope Stage (MIS) 11 has been shown to be a relatively long interglacial period, and is recorded in the Antarctic ice records (EPICA Community Members, 2004), the mid-Asian continent (Prokopenko et al., 2010) and is well recorded in Lake El'gygytgyn (Melles et al., 2012). Focusing on this crucial interglacial offers insight into how future climate changes may affect the planet, as MIS 11 displays similar boundary condition characteristics as found today (Loutre and Berger, 2002), making it a useful analog for modern climate change. Interestingly, Marine Isotope Stage 9 was also an interglacial of particular warmth, yet does not match the ~ 30 ky length of the earlier MIS 11. Analysis of the sediment record through both interglacial periods is intrinsically valuable for understanding the sensitivity of the lake record to global climate changes, and the response of the Russian Arctic to global scale dynamics and change. Additionally, comparing the relative warmth of MIS 9 and MIS 11 to the colder glacial intervals provides the necessary context to evaluate the amplitude of temporal changes expressed around the lake. Knowledge of these past environmental and processes changes then allows for the reconstruction of past climate shifts, which may hold clues for future climate changes.

The work presented here complements research into understanding changes in vegetation surround Lake El'gygytgyn over time. Traditional palynological techniques for reconstructions of terrestrial vegetation (Lozhkin and Anderson, 2013; Lozhkin et al., 2007) are routinely evaluated in conjunction with measures of biogenic silica as an estimation of diatom production and overall productivity (Melles et al., 2012; Vogel et al., 2012). Moreover it is now routine to measure elemental ratios, such as the silica to titanium ratio, as a means to compare clastic input to lake productivity. When these proxies are paired with additional biogeochemical analysis, the magnitude and duration of different interglacial can be evaluated.

The purpose of this thesis is to examine the nature of the MIS 8 through 12 interval, particularly with regards to its duration, as well as the magnitude of precipitation and temperature changes. Records from Lake Baikal demonstrate the extended duration of the MIS 11 interglacial (Prokopenko et al., 2010), and proxy records as well as computer model results from Lake El'gygytgyn demonstrate elevated levels of temperature and precipitation. Furthermore, other studies have recognized unexpected warmth in regards to MIS 10 from the Asian loess plateau (Hao et al., 2013), suggesting more work is needed to understand this critical time period.

In this thesis, multiple proxies for climate changes were utilized, including biomarker investigations, physical sedimentology and mineralogy, sediment color analysis, and sediment geochemistry. By using a suite of various measurements, a more complete understanding of lake processes can be constructed, providing critical information for interpreting the sediment record and its sensitivity to past climate changes.

Biological molecular fossils, otherwise known as biomarkers, are sourced specifically from certain organisms, and provide an in depth analysis of past lake ecological conditions (Castañeda and Schouten, 2011). The ability to identify and quantify lipid markers allows for the quantification of compounds such as dinosterol, specific to dinoflagellates (Withers, 1983, Castaneda and Schouten, 2011), arborinol, a marker for trees (Albrecht and Ourisson, 1969; Jacob et al., 2005), and long chain 1,15 *n*-alkyl diols, which are attributed to eustigmatophyte algae, but likely have additional sources (Volkman et al., 1999, Versteegh et al., 1997; Rampen et al., 2007). In addition, the abundance of glycerol dialkyl glycerol tetraethers (GDGTs), can be calibrated to estimate and reconstruct annual temperatures and soil pH around the lake catchment (Weijers et al., 2007), allowing for ecological reconstructions to be tied with climate parameters. By applying organic geochemical techniques to the MIS 8 – 12 interval, these proxies were used here to demonstrate changes in both the aquatic and terrestrial environment, for comparison with more traditional lake proxies and regional records of change.

In addition to biological proxies, we found it was important to understand the physical and chemical processes at work in the lake catchment in order to properly interpret the sediment record. Rapid core scanning techniques, including reflectance color spectroscopy, can provide non-destructive, high resolution data for the entire 317 meter sediment record. The hue color parameter, calculated from core color measurements (Nowayczyk et al., 2013), revealed shifts in sediment color in conjunction with known climate changes and sediment facies (Melles et al., 2012), and is used here as a proxy for shifts in chemical and physical weathering processes.

In order to validate the use of the hue record on the entire core, detailed analysis of the sediment was conducted across the MIS 8 – 12 interval in order to understand the controls on sediment color. Mineralogical investigations demonstrate changes in bulk mineralogy through time, while clay mineralogy suggested changes in the catchment dominated by physical weathering processes. Fluctuations in mineral content have been shown to drive sediment color (Traschel et al., 2009). Additionally, color sensitivity tests reveal the importance of other sedimentary components such as organic content and iron oxide concentrations, which are known as carriers of distinct color signals (Debret et al., 2011, von Gunten et al., 2011; Deaton and Balsam, 1991). Measurement of the concentrations of iron oxides/hydroxides also provided a means of estimating the relative amount of chemical weathering ongoing in the surrounding catchment, as iron oxides/hydroxides such as hematite and goethite are usually derived from the oxidation of Fe-bearing silicate minerals present in the bedrock encompassing Lake El'gygytgyn. Overall, by linking the hue color record to catchment processes, analysis of how these processes change with regards to interglacial to glacial climate shifts can be furthered understood, and also to demonstrate the use of the hue record as a proxy for chemical and physical chemical processes elsewhere in the core in future studies.

The sediment record from Lake El'gygytgyn provides essential information for understanding of how climate shifts drive lake process changes over time. The aim of this thesis is to compare and contrast multiple climate proxies for the time period including MIS 8 through MIS 12 (~275 ka to ~475ka) in order to investigate the magnitude of interglacial/glacial changes. Investigations into biological proxies demonstrate the elevated warmth of MIS 11 and 9, and support the interpretation of these periods as

"super interglacial" as proposed by Melles et al., (2012). Detailed validation and analysis of the hue color parameter reveal the sediment components that ultimately drive color variations, while also providing a useful proxy for lake catchment processes. By linking color changes to changes in sediment mineralogy, organic content, and secondary iron oxide concentrations, validation and color sensitivity tests allow for the interpretation of the hue record as a proxy for chemical and physical weathering processes. This record not only suggests overall wetter conditions during the interglacial MIS 11 and 9, but also reveals potential periods of enhanced moisture at times outside of interglacial periods. Given the boundary conditions described for these past interglacial periods, the intensity and dynamics of these super-interglacials can be placed into context with contemporary rates of change associated with rising greenhouse gases. These new findings are critical for grasping the magnitude and sensitivity of Arctic regions to climate changes in the past, and like all paleoclimatic studies place the current pace of anthropogenic drive change into much needed context.

1.1 Thesis Outline

This thesis represents two years of Master's research, the results of which are presented in one published manuscript, and another manuscript in preparation. The second chapter, entitled "High-latitude environmental change during MIS 9 & 11: Biogeochemical evidence from Lake El'gygytgyn, Far East Russia", appeared in a special issue of the journal Climate of the Past in early 2013. The manuscript details relatively new biogeochemical techniques used to interpret past climate changes during

the MIS 9 and 11 interglacial periods, and demonstrates the elevated warm conditions of the "super interglacial" periods proposed by Melles et al. (2012).

The third chapter, being developed for publication, covers the geochemical and physical properties of the Lake El'gygytgyn sediment core through the MIS 8 through 12 interval, and the relationship of measured mineralogy and sediment components to high resolution core scanning data sets. Validation of the hue color parameter, which is derived from the high resolution core scans, then offers insights into the processes behind changing sediment color through time, and demonstrates a correspondence of color changes to climate parameters. When coupled with the biogeochemical analyses, a more complete understanding of lake catchment processes can then be developed for the time interval in question.

Chapter IV is a short and final chapter, addressing future research possibilities, given the context from the results of this Master's work. Further investigations building on both the biogeochemical analyses and the understanding of chemical and physical lake processes can be undertaken in the future to forward the knowledge gained from interpreting the Lake El'gygytgyn sediment record. With the unprecedented length and continuity of this sediment record, future investigations are indeed critical for placing both past and future climate changes in context.

CHAPTER 2

HIGH-LATITUDE ENVIRONMENTAL CHANGE DURING MIS 9 & 11: BIOGEOCHEMICAL EVIDENCE FROM LAKE EL'GYGYTGYN, FAR EAST RUSSIA

Robert M. D'Anjou, Jeremy H. Wei, Isla S. Castañeda, Julie Brigham-Grette, Steven T. Petsch & David B. Finkelstein

Climate of the Past, 9, 567-581, 2013

Climate Systems Research Center and Department of Geosciences, University of Massachusetts Amherst, Amherst, MA, 01003
(E-Mail: rdanjou@geo.umass.edu)

2.1 Abstract

Marine Isotope Stages (MIS) 11 has been proposed as an analog for the present interglacial; however, terrestrial records of this time period are rare. Sediments from Lake El'gygytgyn (67°30'N, 172°5'E) in Far East Russia contain a 3.56 Ma record of climate variability from the Arctic. Here, we present the first terrestrial Arctic reconstruction of environmental and climatic changes from MIS 8 through 12 (289 to 464 ka) using organic geochemical proxies. Terrestrial vegetation changes, as revealed by plant leaf wax (*n*-alkane) indices and concentrations of arborinol (a biomarker for trees), show increased tree cover around the lake during interglacial periods, with higher concentrations observed during MIS 11 as compared to MIS 9. A similar pattern is also observed in records of aquatic productivity revealed by molecular indicators from dinoflagellates (dinosterol), eustigmatophyte algae (long-chain (C_{28}-C_{32}) 1,15 *n*-alkyl diols) in addition to short-chain *n*-alkanes, where aquatic productivity is highest during MIS 11. Changes recorded in these molecular proxies show a similar structure to relative temperature variability as recorded by the MBT/CBT paleothermometer, based on

branched glycerol dialkyl glycerol tetraethers (GDGTs). Additionally, relative MBT/CBT temperature changes generally track pollen and diatom $\delta^{18}O$ temperature estimates, compiled by other studies, which suggest glacial-interglacial temperature changes of ~ 9 to 12°C. These records of environmental and climatic change indicate Arctic sensitivity to external forcings such as orbital variability and atmospheric greenhouse gas concentrations. Overall, this study indicates that organic geochemical analyses of the Lake El'gygytgyn sediment archive can provide critical insight into the response of lake ecosystems and their sensitivity in high latitude regions.

2.2 Introduction

Marine Isotope Stage (MIS) 11 has been proposed as an analog to modern climate conditions, with orbital configurations similar to today and greenhouse gas concentrations at pre-industrial levels (Loutre and Berger, 2002; EPICA community members, 2004). Past studies indicate that MIS 11 was one of the warmest and longest interglacial periods of the past 5 Ma. The characteristics of this "super" interglacial (Melles et al., 2012) period have been expressed globally in North Atlantic marine sediment core records (Voelker et al., 2010; Lawrence et al., 2010), as well as in Asian lacustrine sedimentary records from Lake Baikal, which indicate a prolonged interglacial period of ~30 ky (Prokopenko et al, 2010). However, terrestrial records from high latitude regions of the Asian continent are almost non-existent, yet can play a crucial role in understanding aspects of the climate system that currently are not well characterized. The sediment record obtained from Lake El'gygytgyn in Far East Arctic Russia contains a continuous archive of climate variability since the middle Pliocene and permits critical

analysis of the structure, and corresponding response of this Western Beringian ecosystem to changes during the MIS 11 "super" interglacial period.

The interval spanning MIS stages 9 through 12 is of particular interest to paleoclimatic studies as higher magnitude glacial-interglacial transitions, such as the MIS 12 to MIS 11(Termination V) transition, was of larger magnitude when compared to previous glacial-interglacial transitions (EPICA community members, 2004). During the peak warmth of MIS 11, global sea levels are understood to have been significantly higher than other interglacials over the past 400,000 years possibly due to significant collapse of both the Greenland Ice sheet and the West Antarctic Ice Sheet (Raymo and Mitrovica, 2012). This interval, known as the Mid-Bruhnes transition, marks a period when the amplitude of interglacial – glacial variability increases following ~ 430 ka. Furthermore, past studies on Lake El'gygytgyn sediments by Melles et al. (2012), label MIS 11c as a "super" interglacial where lake sediments reflect high diatom and terrestrial plant productivity.

In this study we examine biogeochemical processes in Lake El'gygytgyn during the period of MIS 9 through 11 (289 to 464 ka) using multiple organic geochemical-based proxies. Specifically, this study uses organic biomarkers in lake sediments as proxies for reconstructing changes in past environmental conditions. Here, we estimate relative temperature changes using the MBT/CBT (Methylation of Branched Tetraether/ Cyclization of Branched Tetraether) paleothermometer (Table 1), which relates changes in the degree of methylation and cyclisation of branched glycerol dialkyl glycerol tetraethers (brGDGTS) to mean annual air temperature and pH (Weijers et al., 2007b). Compounds specific to trees and aquatic organisms demonstrate variability in terrestrial

vegetation and aquatic inputs through time, and show responses to changing climate regimes. Finally, our record is comparable to published records from both marine and terrestrial settings, fitting the Lake El'gygytgyn record into a global context. This paper complements the focused summary of other proxies from MIS 11 reviewed by Vogel et al. (this volume).

2.3 Background Information

2.3.1 Lake Catchment and Site Description

Lake El'gygytgyn is located in the Chukotka Peninsula in the Far East Russian Arctic (67°30'N, 172°5'E) (Figure 1). The catchment area sits in an impact structure formed at 3.58 +/- .04 Ma (Layer, 2000), with a rim-to-rim diameter of 18 km and a catchment area of approximately 293 km^2 (Nolan & Brigham-Grette, 2007). A network of 50 streams carries surface runoff into the lake, and the Enmyvaam River serves as the outlet to the Bering Sea (Nolan and Brigham-Grette, 2007). Lake El'gygytgyn is seated within the bottom of this crater, and is 12 km wide and 175 m deep with an approximate volume of 14.1 km^3 (Nolan and Brigham-Grette, 2007). The lake is an oligotrophic and monomictic lake, with modern lake temperatures which do not exceed 4° C and with annual overturning in late summer (Nolan and Brigham-Grette, 2007). Lake ice formation occurs by October, and persists to July.

Modern air temperatures at the lake range from -46 °C in the winter to as high as +26 °C in summer with a mean annual temperature of -10.3°C (Nolan and Brigham-Grette, 2007). Precipitation levels are generally low, with cumulative precipitation from

2002 to 2007 ranging from 70 to 200 mm (Nolan, 2012). Strong winds also affect the El'gygytgyn area, with dominant directions out of the north or south and strongest winds in winter (Nolan and Brigham-Grette, 2007). The modern vegetation around the lake can be characterized as arctic tundra consisting of lichen and herbaceous taxa (Lozhkin et al., 2007). Around the high-relief slopes of the catchment basin this flora is often limited and discontinuous. The closest modern day forests lie ~150 km SW of the lake, occurring as light conifer forest (Lozhkin et al., 2007).

2.3.2 Chronology

Sediment used by this study was taken from ICDP core 5011-1 (Figure 1), extracted from Lake El'gygytgyn in 2009. Thirty-nine samples were taken at varying depth intervals between 13.9 m and 20.7 m with each sample representing ~500 to 1000 years. The composite core (Wennrich et al., this volume) record was tuned from fixed tie points based on magnetostratigraphic investigations and the ages of magnetic reversals from Lisiecki and Raymo (2005), which has a reported error of 4 ky for the 0-1 Ma interval. This work and synchronous tuning of 9 data sets between the magnetic tie points is reported in Melles et al., (2012). Due to a sediment slump feature in the ICDP core during MIS 10, the samples from MIS 11 (21 samples) were furthered shifted by approximately ~ 2000 years to compensate for missing time in the sediment record, well within the error of the Lisiecki and Raymo (2005) benthic stack, and the Lake El'gygytgyn age models.

2.3.3 Biomarkers

Various classes of organic molecules (lipids) have been extensively studied and proven to be useful biomarkers due to their relative resistance to degradation and source specific molecular configurations (e.g. Eglinton and Hamilton, 1967; Volkman, 1987; Cranwell, 1973). In this paleolimnological study, the lipid compound classes of aliphatic hydrocarbons (*n*-alkanes), long chain 1,15 *n*-alkyl diols, sterols, pentacyclic triterpenes and glycerol dialkyl glycerol tetraethers (GDGTs) have been identified, quantified, and used to examine variability in terrestrial and aquatic community structures during MIS 9 and 11. Using records of these compound classes produced in and around Lake El'gygytgyn, we investigate the relationship between changes in chemical remains preserved in the lacustrine sedimentary record and climatic changes during this critical period of time.

Aliphatic hydrocarbons (*n*-alkanes) are organic compounds derived from both autochthonous and allochthonous sources (e.g. Eglinton and Hamilton, 1967; Didyk et al., 1978; Meyers and Ishiwatari, 1993) and are widespread biomarkers in lacustrine sedimentary archives. The principal sources of biogenic aliphatic hydrocarbons to lake sediments are algae, bacteria and vascular plants that live within a lake, and vascular plants that live around it. These compounds are often used as recorders of local environmental changes. Short chain *n*-alkanes C_{15}-C_{21} (especially C_{17}) are attributed to algae and photosynthetic bacteria (e.g. Cranwell et al., 1987; Meyers, 2003 and references therein), submerged and emergent aquatic plants are the main producers of mid-chain (C_{21}, C_{23}, and C_{25}) *n*-alkanes (Ficken et al., 2000), while long-chain homologues (C_{25}-C_{33}) are characteristic of higher order terrestrial plants (e.g. Eglinton

and Hamilton, 1967; Cranwell et al., 1987). The *n*-alkane indices such as the Terrestrial to Aquatic Ratio (TAR) (Bourbonniere and Meyers, 1997) and the Carbon Preference Index (CPI) (Bray and Evans, 1961) (Table 1) can provide important constraints on the characteristic molecular distributions in each sample; these indices can reveal trends in the patterns and distributions of short-to-long carbon chain number and odd-to-even carbon number predominance in the *n*-alkane profiles from our lake sediment samples. The *n*-alkane CPI can provide information on both preservation/degradation patterns in sedimentary records and/or source organism distributions helping to differentiate contributions from terrestrial, aquatic, and bacterial sources, with terrestrial sources usually showing the highest CPI values, followed by aquatic, and then bacterial sources (Bray and Evans, 1961; Eglinton and Hamilton, 1967). The *n*-alkane TAR index can provide useful information on organic matter (OM) sources, helping to distinguish the contributions of land-derived OM from that of aquatic sources, using the basic premise of carbon chain length variations specific to organism sources (Bourbonniere and Meyers, 1997).

Compounds such as sterols (and their saturated analogs, stanols) are useful biomarkers because carbon number, position of methyl groups, and double bonds in the molecule are indicative of certain groups of organisms (Volkman, 1986, 2003; Volkman et al., 1998). For example, dinoflagellate (Pyrrophyta) species are characterized by high concentrations of 4α-methyl sterols with dinosterol (4α,23,24-trimethyl-5α-cholest-22-en-3β-ol) as the main constituent in some species (Withers, 1983). Additionally, dinosterol is not known to be produced from terrestrial sources and is relatively absent from other aquatic species (Volkman, 1986). However, it has been noted that dinosterol is

not necessarily produced by all species of dinoflagellates (Rampen et al., 2010). Nevertheless, dinosterol has been extensively used as a biomarker for dinoflagellates (Castañeda and Schouten, 2011 and references therein), and is useful for examining past changes in dinoflagellate productivity (e.g. Castañeda et al., 2011).

The presence of long-chain (C_{28} - C_{32}) 1,15 *n*-alkyl diols in lake sediments may indicate input from algae, as these compounds are common constituents of marine sediments where they are thought to be produced by Eustigmatophyte algae (Volkman et al., 1992, 1999; Versteegh et al., 1997; Rampen et al., 2007, 2008) although we note that other producers may exist in lakes (Castañeda and Schouten, 2011 and references therein). Long-chain (C_{28-32}) 1,15 *n*-alkyl diols have been detected in a variety of marine and freshwater sediments (Castañeda et al., 2009 and references therein) and these compounds can be used to reconstruct aquatic primary productivity within lacustrine systems, which has been shown to have the potential for tracking climatic and environmental variability.

Pentacyclic triterpenes and their respective derivatives such as arborinol (arbor-9(11)-en-3a-ol) are characteristic triterpenes of higher-order terrestrial vegetation (Albrecht and Ourisson, 1969; Vliex et al., 1994; Jacobs et al., 2005). Specifically, arborinol has been extracted from the leaves of numerous species of trees, and can provide a record of changes in the extent of forest cover in an area (Jacobs et al., 2005, and references therein).

Branched GDGTs (brGDGTs) are commonly found in soils and peats and are believed to be produced by anaerobic soil bacteria although the source organism(s) presently remains unknown (Weijers et al., 2007b). Acidobacteria are another possible

source of brGDGTs in soils, as it has been shown that in laboratory cultures, some strains produce the brGDGT-I compound (Sinninghe Damsté et al., 2011). Changes in the degree of methylation (MBT) and cyclization (CBT) of branched GDGTs (Table I) are a temperature and pH dependent process (Weijers et al., 2007b) and the MBT/CBT paleothermometer has been used to examine past continental temperature variability (e.g. Weijers et al., 2007a; Fawcett et al., 2011). The main source of brGDGTs to marine settings is generally fluvial transport and thus MBT/CBT-derived temperatures can represent the mean annual air (soil) temperature of the river drainage (e.g. Weijers et al., 2007b). In lacustrine systems application of the MBT/CBT paleothermometer is not as straightforward (Castañeda and Schouten, 2011) as there is strong evidence that brGDGTs can also be produced in-situ from within the water column (Peterse et al., 2009; Tierney and Russell, 2009; Sinninghe Damsté et al., 2009; Bechtel et al., 2010; Blaga et al., 2010; Tierney et al., 2012). Despite uncertainties pertaining to the origin of brGDGTs in lake sediments, several studies have applied the MBT/CBT paleothermometer to sediment cores to examine past temperature variability (e.g. Zink et al., 2010; Fawcett et al., 2011; Blaga et al., 2011). It should be noted that regional or lake specific calibrations are likely needed when applying the MBT/CBT paleothermometer to lakes (e.g. Tierney et al., 2010; Zink et al., 2010; Castañeda and Schouten, 2011) and without a site-specific calibration, MBT/CBT-derived temperatures should only be interpreted in terms of relative temperature change and not absolute temperatures.

2.4 Methods

2.4.1 Sample Extraction

Thirty-nine sediment samples (~ 6-12g) were selected for molecular analyses at a coarse sampling resolution of ~one sample per 10 ky for the 200 ky study interval, which spans from 289 to 464 ka. Freeze dried, homogenized sediment samples were extracted with dichloromethane/methanol (9:1, v/v) mixture at a temperature of 100°C , using a Dionex Automated Solvent Extractor (ASE). The results of this study represent processing of samples at different times using slightly different methods. For 26 of the samples, the total lipid extract was split in half and one half was separated into five fractions by silica-gel column-chromatography: (F1) aliphatic hydrocarbons (hexane), (F2) ketones (4:1 hexane:DCM, vol:vol), (F3) *n*-alkanols/sterols/stanols (9:1 DCM:acetone vol:vol), (F4) fatty acids (2% formic acid in DCM) and (F5) polar compounds (methanol). For the remaining half of the TLE from these 26 samples along with 13 additional samples, the TLE was separated into apolar (9:1 DCM:hexane, vol/vol), ketone (1:1 DCM:hexane, vol/vol) and polar (1:1 DCM:MeOH, vol/vol) fractions using alumina oxide column chromatography. One sample at ~460 ka (480ka) was not included in the brGDGT analysis due to complications in laboratory procedures, however was processed for all other analyses. The *n*-alkanol/sterol/stanol fraction (F3) and the polar fractions from the first and second column schemes, were derivitized to their trimethylsilyl-ethers using bistrimethylsilyltrifluoroacetamide (BSTFA) with acetonitrile as a catalyst (1:1, V:V) at 60–70°C for roughly one hour prior to GC analysis.

2.4.2 Compound Identification and Quantification by GC and HC-MS

Compound identification was performed using a Hewlett Packard 6890 series gas chromatograph (GC)– mass spectrometer equipped with a 5% phenyl methyl siloxane column (HP-5, 60m x 0.25mm x 0.25µm). The GC-MS oven temperature program for

running the F1/apolar and the F3/polar fractions initiated at 70°C, increased at a rate of 20 °C min^{-1} to 130 °C and then next increased at a rate of 4 °C min^{-1} to 320°C. The final temperature of 320°C was held for 20 min. Mass scans were made over the interval from 50 to 600 m/z. Compound identification was achieved by interpretation of characteristic mass spectra fragmentation patterns, gas chromatographic relative retention times, and by comparison with literature.

Quantification was performed using a Hewlett Packard 6890 series GC-Flame Ionization Detector (GC-FID) equipped with the same capillary column and using the same temperature program as described above. Compound concentrations were calculated by comparing integrated sample peak areas with the integrated peak areas of an added internal standard (hexatriacontane, the C_{37} *n*-alkane) .

2.4.3 Compound Identification and Quantification by HPLC – MS

Splits of the polar fractions were filtered through a 0.45 µm PTFE syringe filter in 99:1 hexane:propanol (vol/vol) and were subsequently analyzed on an Agilent 1260 HPLC coupled to an Agilent 6120 MSD, for identification and quantification GDGTs following the methods of Hopmans et al. (2000), with minor modifications (Schouten et al., 2007). A C_{46} GDGT was used as an internal standard. Separation was achieved on a Prevail Cyano column (150 mm × 2.1 mm, 3 µm) using 99:1 hexane:propanol (vol:vol) as an eluent. After the first 7 min, the eluent increased by a linear gradient up to 1.8% isopropanol (vol) over the next 45 min at a flow rate of 0.2 ml min^{-1}. Scanning was performed in selected ion monitoring (SIM) mode.

2.5 Results

$C_{28,}$ C_{30} and C_{32} *n*-alkyl 1,15-diols are present in high concentrations during interglacial periods MIS 9 and 11 (Figure 2B) with total concentrations (sum of C_{28}, C_{30} and C_{32} 1,15 *n*-alkyl diols) ranging from 1.16 to 20.17 µg g_{sed}^{-1} and average concentrations of 9.30 and 16.25 µg g_{sed}^{-1} for MIS 9 and 11, respectively. During glacial periods long-chain 1,15 *n*-alkyl-diols are present in low concentrations (Figure 2B), with total concentrations ranging from 0.92 to 4.97 µg g_{sed}^{-1} and averages of 2.22, 1.39 and 3.01 µg g_{sed}^{-1} for MIS 8, 10 and 12, respectively.

Dinosterol concentrations show a similar overall trend to those of the long-chain 1,15 *n*-alkyl-diols, with relatively high average concentrations of 3.18 and 4.08 µg g_{sed}^{-1} during respective interglacial stages 9 and 11 (Figure 2D), while present in very low concentrations during glacial periods with average concentrations of 0.38, 0.41 and 0.57 µg g_{sed}^{-1} for MIS 8, 10 and 12 respectively. Arborinol concentrations are highest during interglacial periods (MIS 9 and 11; Figure 2C) varying in concentration between 1.69 and 28.53 µg g_{sed}^{-1} with an average concentration of 13.57 and 21.63 µg g_{sed}^{-1} during MIS 9 and 11, respectively. Arborinol concentrations drop off rapidly during interglacial to glacial transitions, and are below detection limits during most of the glacial periods (MIS 8, 10, and 12) varying between 0 and 4.14 µg g sed^{-1} with an average concentration of 1.69 µg g_{sed}^{-1} for all glacial periods.

Branched GDGT concentrations range from 0.09 to 0.99 µg g_{sed}^{-1} and on average are more abundant during interglacial periods (Figure 2E). MBT/CBT derived temperature estimates range from -9.2 to 3.0 °C when applying the global soils calibration of Weijers et al. (2007b) and from -3.5 to 6.4°C when applying the

MBT'/CBT soils calibration of Peterse et al. (2012). Using other published lacustrine calibrations, the temperatures range from 6.7 to 16.5°C (Tierney et al., 2010), 8.1 to 17.9 °C (Pearson et al., 2011), 1.4 to 13.4°C (Sun et al., 2011) and 0.2 to 9.8°C (Zink et al., 2010) (Figure 3A-F). The lowest temperature according to the Weijers et al. (2007b) calibration is noted at 440 ka (MIS 12) while the highest value occurs ~25 ky later, at 415 ka (MIS 11).

Carbon numbers for *n*-alkanes range from C_{17} to C_{35}. Carbon-preference index values (CPI) for C_{23} to C_{33} *n*-alkanes show values between 1.8 and 6.1 for all sample depths, with an average of 3.1$\pm$0.7 (Figure 3J). The terrestrial to aquatic *n*-alkane ratio (TAR) has values between 1.07 and 7.59, with an average value of 3.72 (Figure 3I). The carbon number with the maximum abundance varies considerably between samples, with some samples having bimodal distributions peaking at C_{17} and C_{27}, C_{29}, or C_{31}, and others showing a monomodal distribution with a single maximum at C_{27}, C_{29} or C_{31}. Average chain lengths (ACL) (Poynter and Eglinton, 1990) range from 25 to 28 (not plotted) but do not show distinct patterns between all glacial and interglacial periods.

2.6 Discussion

Previous studies of Lake El'gygytgyn point toward both a global and regional response of the lake environment to various climate forcings (Lozhkin et al., 2007; Melles et al, 2007; Melles et al., 2012). A record of pollen counts and diatom productivity (the latter inferred from the Si/Ti record as shown by Melles et al. (2012); Figure 4D.) shows the highest terrestrial and aquatic productivity during MIS 11, while MIS 9 is characterized by slightly diminished productivity relative to MIS 11 (Melles et

al., 2012). The overall paleo-environmental record presented here corroborates past work, and our results further elucidate subtle differences in ecological community structure and productivity during MIS 9 and MIS 11. Temperatures recorded by the MBT/CBT paleothermometer are often correlated strongly with other biogeochemical proxy records of terrestrial vegetation changes and aquatic productivity, showing a clear response of each to local temperature variability during interglacial-glacial transitions as well as within interglacial periods. Biogeochemical proxy records also show a high degree of correlation with various other paleorecords such as those from continental Asia (Lake Baikal), the Bering Sea, the North Atlantic, and Antarctica, indicating an integrated global response (Figure 4, cf Vogel et al., this volume).

2.6.1 Biogeochemical Records and Normalization

The percent of total organic carbon (%TOC) may be used as a proxy for primary productivity in lakes (Meyers and Ishiwatari 1993; 1995; Meyers, 1997) although TOC in lacustrine sediments represents contributions from both autochthonous and allochthonous sources. Overall %TOC values in Lake El'gygytgyn are low and range from 0.1-3 % over the interval of study, reflecting the monomictic oligotrophic to ultra-oligotrophic nature of the lake (Melles et al., 2012). Interestingly, we note that the response of TOC in Lake El' gygytgyn during Quaternary glacial and interglacial periods is not consistent throughout the record (Figure 3G), and the mechanisms behind this variability are not well characterized. An example of the variable nature of the TOC record occurs during the MIS 2 glacial period, where %TOC is much higher than during the two surrounding interglacial periods, MIS 1 and 3 (Holland et al., 2013). The TOC data from MIS 9 and 11 reveal a somewhat contrasting response with slightly elevated TOC values during MIS

11 in comparison to the surrounding glacials, MIS 10 and 12 (Figure 3G). However, TOC data from MIS 9 cannot readily be demarcated from the surrounding interglacials MIS 8 and 10, as they are all characterized by relatively similar values. In contrast, all other biological based proxies from Lake El'gygytgyn (ie biogenic silica) clearly show elevated values corresponding to interglacial periods throughout the Pleistocene, including MIS 9 and 11(Figure 4H), making them easily discernible from the surrounding glacial periods. Although normalizing biogeochemical data to grams of organic carbon using %TOC values is a common method to investigate the effects of preservation vs. production on biomarker concentrations, the nature of TOC data in Lake El'gygytgyn, especially during MIS 9 and 11, prevents the confident use of the TOC data to normalize the biomarker data. Ongoing organic geochemical suggests that the non-solvent extractable portion of TOC varies considerably, and independently of glacial/interglacial cycles, at Lake El'gygytgyn. As such, the biomarker concentration data is normalized to g sediment extracted (g_{sed}^{-1}).

2.6.2 Preservation of Organic Matter

The CPI is often used to examine preservation of OM, yet the relationship between *n*-alkane CPI values and degradation is less clear in aquatic environments due to the weaker odd over even preference of bacteria and aquatic algae (Grimalt & Albaiges, 1987) that results in lower CPI values compared to terrestrial OM (Cranwell et al., 1987). OM in aquatic sediments is usually considered substantially degraded when CPI values are below 1 (Bray and Evans, 1961) Because CPI values of *n*-alkanes (1.8–6.1) are higher than 1 throughout this record (avg.= 3.1$\pm$0.7), and there are no observable trends in

decreasing CPI down-core, progressive OM biodegradation through time is likely to be limited in this record. However, it has been proposed that the bottom waters of Lake El'gygytgyn become anoxic/suboxic during various glacial periods, in which case OM degradation may have had a greater influence on the preservation of OM in the lake throughout glacial/interglacial transitions (Holland et al., 2013). During interglacial periods (MIS 9 and 11) the CPI record exhibits the highest values, which quickly drop off to significantly lower values as the record transitions to glacial periods (MIS 8, 10 and 12). This trend can be attributed to either a decrease in biodegradation of OM during interglacial periods or it otherwise may represent an increase in terrestrial OM input. However, based on our records we do not have the necessary information to designate the relative amounts either of these mechanisms may have had on the observed trends in CPI and OM preservation.

2.6.3 Temperature Variability

Relative temperature changes at Lake El'gygytgyn were examined using the MBT/CBT paleothermometer by applying several different calibrations (Weijers et al., 2007b; Tierney et al., 2010; Zink et al., 2010; Pearson et al., 2011;Sun et al., 2011; Peterse et al., 2012) (Figure 3A-F). We note that without a modern calibration set and without knowing if the main source of brGDGTs in Lake El'gygytgyn is from within the lake or the watershed, it is not clear which of the presently available MBT/CBT calibrations is the most suitable to apply. It has been suggested that site specific or regional calibrations may be needed for MBT/CBT and other factors such as a seasonal

production maximum of brGDGTs should be evaluated for individual sites (Castañeda and Schouten, 2011). We note modern air temperatures at this site span from -40 to +26°C, with a mean annual air temperature of -10.3°C (Nolan and Brigham-Grette, 2007). Water temperatures within the lake are always below 4°C, although shallow shelf areas can reach up to 5°C in summer (Nolan and Brigham-Grette, 2007). Palynological data from Lake El'gygytgyn sediment cores has been previously used to calculate the mean temperature of the warmest month (MTWM) based on terrestrial vegetation pollen assemblage abundances over the MIS 11 to MIS 12 transition, and reveal a ~12°C relative temperature change during this period (Melles et al., 2012). Furthermore, temperature estimates from diatom $\delta^{18}O$ (Chapligin et al., this volume) suggest interglacial to glacial changes of ~9°C, both of which support interglacial to glacial temperature changes which are similar to ranges reported from the multiple MBT/CBT reconstructions. Yet given the wide range of temperatures noted in and around the lake, all of the currently available MBT/CBT calibrations to temperature could be feasible, especially if seasonal biases are considered. Therefore, at present, absolute temperatures as recorded by MBT/CBT cannot be reconstructed with confidence at Lake El'gygytgyn. Noteably, MBT/CBT indices shown in Figures 3A and 3B are similar to the MTWM index compiled by Tarasov in Melles et al. (2012).

In marine settings, the Branched and Isoprenoid Tetraether (BIT) Index (Hopmans et al., 2004) provides a proxy for soil organic matter versus aquatic input and is based on a ratio of relative abundances of brGDGTs to crenarchaeol, a biomarker of aquatic thaumarchaeota (formerly crenarchaeota). BIT index values range from 0 to 1, with an aquatic end member value of 0 indicating an aquatic end member in which

crenarchaeol is the only compound present, while a value of 1 represents pure soil OM source (Hopmans et al., 2004). However, in lakes the interpretation of BIT index values is not as straightforward as brGDGTs likely also derive from within the water column (Peterse et al., 2009; Tierney and Russell, 2009; Sinninghe Damsté et al., 2009; Bechtel et al., 2010; Blaga et al., 2010; Tierney et al., 2012). At Lake El'gygytgyn, BIT values are quite high and range from 0.74 to 0.99 (Figure 2F) during MIS 8 to 12 but are driven mainly by variations in crenarchaeol concentrations rather than by variations in inputs of brGDGTs. Lower BIT index values (Figure 2F) correlate to intervals when increased concentrations of crenarchaeol are noted (Figure 2G).

For the reasons stated above, we strongly caution readers against interpreting Lake El'gygytgyn MBT/CBT derived temperatures either in terms of absolute temperatures or the overall amplitude of the temperature signal. However, relative temperature changes from the MBT/CBT record are presented and show varying degrees of correspondence with summer insolation for 67.5° N (Figure 4F). A comparison to local insolation (Laskar et al., 2004) shows some similarities, suggesting that MBT/CBT-derived temperatures could represent a signal of summer temperature, a concept previously proposed by Pearson et al. (2011), although some of the differences between the MBT/CBT record and insolation could arise as a result of the large uncertainties inherent in the age model used. Furthermore, the MBT/CBT temperatures demonstrate changes resembling interstadial periods MIS 11.b and MIS 9.b (Figures 3A-F), which is indicative of the potential sensitivity of the MBT/CBT method. Yet, given the sampling resolution of this study, interglacial subdivisions are speculative and merely resemble subdivision made in previous studies (Lisiecki and Raymo, 2005).Higher resolution analyses for this interval

are required before further interpretations can be made, but the 30 ka duration of the MIS 11 interglacial shown by Prokopenko et al. (2010) in Lake Baikal records is nevertheless evident in our record. During the MIS 10 glacial period, MBT/CBT- derived temperature estimates are anomalously high in three of the samples (Figures 3A-F). The high variability exhibited in samples from the MIS 10 is not well understood, although variability in summer insolation is a possible explanation. Hao et al. (2013) also demonstrate a weakening of the East Asian winter monsoon, and therefore a weaker Siberian High, during MIS 10. This weakening would result in persistent non glacial conditions during MIS 10 based on records from the Chinese Loess Plateau, providing a different potential mechanism for the warmth recorded by the MBT/CBT proxy at this time.

2.6.4 Vegetation Change

During the MIS 11 interglacial, values for the *n*-alkane indices (CPI and TAR) suggest OM in the sediment is largely from terrestrial sources, a trend that is corroborated by tree pollen records and high arborinol concentrations (Figure 2C), suggesting forestation of the lake catchment (Melles et al., 2012, Lozhkin and Anderson, this volume). This is likely a result of increased sensitivity of terrestrial vegetation in Arctic regions, as a drop in temperature can easily cause permanent snow and nivation hollows to form, killing off most terrestrial vegetation, while submerged aquatic plants and bacteria can continue to thrive as long as sunlight can still penetrate the ice-cover (Melles et al., 2007). The interpretations made from the *n*-alkane CPI record are further supported by the *n*-alkane TAR proxy, revealing changes in the amount of OM being delivered

from terrigenous or aquatic sources. Mean *n*-alkane TAR values suggest higher overall terrestrial contributions in MIS 11.

Following peak warmth at 415 ka, vegetation records based on arborinol concentrations and pollen data exhibit a gradual decrease in terrestrial vegetation, especially after the drop in temperature at ~400 ka (MIS 11.b) before the onset of MIS 10 (Figure 4A, 4B). During the glacial interval at ~ 395 ka, arborinol concentrations are at or below the detection limit, indicative of the return of tundra plant cover and/permanent snow cover.

The response of the terrestrial and aquatic communities to MIS 9 is somewhat weaker from that of MIS 11, supporting previous observations by Melles et al. (2012) that MIS 11 was a "super interglacial" period. Biomarker data from MIS 9 indicate a clear interval of warmth (Figures 2-4). Early in MIS 9, warmer interglacial MBT/CBT-derived temperatures suggest that the terrestrial community may have experienced full forestation, supported by the high concentrations of arborinol, and low CPI values during this time period (325 to 335 ka). Pollen records from the MIS 9 time period (Lozhkin et al., 2007b), together with the record of arborinol, indicates MIS 9 overall was a weaker interglacial than MIS 11. The highest terrestrial productivity based on the Si/Ti ratio also coincides with the period of peak MIS 9 warmth as recorded by the MBT/CBT record, indicating the growth of trees and shrubs with warmer temperatures (Figures 3 and 4).

Possible explanations for the vegetation differences include variability of both summer insolation and CO_2 during MIS 9 and11 (Laskar, 2004; EPICA Community Members, 2004). Although peak CO_2 and insolation values are both highest in MIS 9, MIS 11 records indicate slightly lower yet less variable CO_2 and insolation values. These

stable forcings could have resulted in the higher vegetation response; otherwise this could have also resulted from changes in preservation, if for instance, there was increased anoxia during MIS 11. Although records from later glacial periods such as the Last Glacial Maximum (MIS 2) show higher TOC and biomarker concentrations than interglacials (MIS 1 and 3)(Holland et al., 2013), recent work has also demonstrated that OM preservation/degradation during MIS 2 is an anomalous interval, for the period spanning 0 to 1.2 Ma (Snyder et al., this volume). Therefore, MIS 2 may not serve as a good analog for other interglacial and glacial period from deeper parts of the Lake El'gygytgyn record.

2.6.5 Aquatic Productivity

At Lake El'gygytgyn, stable and warm temperatures during interglacials could have allowed for increased aquatic productivity and diversity, a point corroborated by high concentrations of the aquatic biomarkers of long-chain 1,15 *n*-alkyl-diols, dinosterol, and diatom productivity as indicated by the lake Si/Ti ratio proxy (Melles et al., 2012). These increases in biomarker concentrations may also reflect increases in the preservation of organic matter due to changes in dynamics of the lake operating system as a response to climatic changes (Snyder et al., this volume). During peak MIS 11 (420 to 400 ka), the concentrations of the aquatic biomarkers reach the highest values of the record (Figures 2A), which correspond with a period (418.5 to 402 ka) of peak warmth and precipitation determined by Vogel et al. (2012). At the 400 ka temperature drop recorded by MBT/CBT, CPI values decrease rapidly, and slight decreases in long-chain 1,15 *n*-alkyl-diols and dinosterol concentrations are evident (Figure 2B). Following this

temperature drop, our biomarker records indicate a rebound in the dinoflagellate and algal communities, with higher productivity prior to the onset of MIS 10 while Si/Ti ratios (an indicator of diatom productivity) fail to recover. The lack of diatoms and high concentrations of dinosterol and long-chain 1,15 *n*-alkyl-diols points to biological niche conditions where decreasing temperatures are coincident with less diversity of primary producers in the lake water, as opposed to peak MIS 11 warm conditions where the lake supports a diverse aquatic community of primary producer organisms. While our records do not show evidence for a strong glacial/interglacial change in the preservation of OM in Lake El'gygytgyn, it is possible that preservation during glacial versus interglacial periods is in fact different. If so, biomarker concentrations in our records may show biases based on preservation rates, especially when making glacial to interglacial comparisons (Holland et al., 2013).

We searched for the compounds loliolide, isololiolide, gorgesterol, fucoxanthin, and various methyl-cholesterol compounds, all of which have been used as molecular indicators for the presence of different diatom species communities (Rampen et al., 2010). Despite biogenic silica records indicating the presence of a substantial diatom community in Lake El'gygytgyn, thus far, we have been unable to identify any of these diagnostic molecular markers in our sediment samples.

2.6.6 MIS 9 and 11 Interglacial Comparisons

Overall, biomarker records indicate high temperatures during MIS 11.c, and warm temperatures during MIS 9 as suggested by the MBT/CBT paleothermometer. As such, the climate both of MIS 11.c and MIS 9 supported a diverse range of organisms,

including high productivity of terrestrial plants as well as high numbers of diatoms, dinoflagellates, and algal organisms (cf. Snyder et al., this volume). The transition from interglacial to glacial periods is marked by a dramatically sharp decline in long chain 1,15 *n*-alkyl diols (Figure 2B), indicating that a critical threshold was reached.

Following MIS 10 glaciation, GDGT temperatures show evidence for a single warm periods occurring during MIS 9 (Figure 3). Temperatures during early MIS 9 reveal a warm peak associated with increased diatom, algal, and terrestrial productivity. The aquatic community is similar to the MIS 11 peak, where high concentrations of all aquatic markers, abundant diatoms and an increase in sediment accumulation rates were measured (Snyder et al., 2012; Cunningham et al., 2012). The record of long-chain (C_{28} - C_{32}) 1,15 *n*-alkyl diols suggests elevated contributions from eustigmatophyte algae as well, although these compounds are not present at the higher values measured for MIS 11. Early MIS 9 resembles the community structure of late MIS 11 following the 400 ka temperature drop where diatom abundance decreased but dinoflagellate levels remained high. Recorded changes in aquatic productivity are similar to our records of terrestrial vegetation variability, and the two demonstrate a high degree of correlation (Figure 2A). In this sense, aquatic productivity further substantiates how the lake and catchment area has responded to stable versus more variable climate forcings in the past.

2.6.7 Global Context

Orbital parameters vary notably between MIS 11 and MIS 9 (Yin and Berger, 2010), as evident in the July insolation curve at 67.5° N (Laskar, 2004) (Figure 4G.). Discrepancies in local insolation during these periods are one possible mechanistic

explanation for the observed variability of local temperatures estimated by the MBT/CBT index. Yet during these two interglacial periods there are also differences in global atmospheric concentrations of CO_2 , with average concentrations at ~260 ppm and 270 ppm during MIS 9 and 11, respectively (EPICA Community Members, 2004). The slightly higher and more stable average atmospheric concentrations of global CO_2 during MIS 11 present a possible mechanism behind the distinctively warm and stable conditions that characterize the MIS 11 interglacial period in our records even though total insolation is less than that of MIS 9 by ~ 20 W/m^2 (Laskar, 2004). While MIS 9 peak atmospheric CO_2 levels were higher than during MIS 11 (Luthi et al., 2008), the stability and duration of elevated CO_2 concentrations during MIS 11 results in higher average CO_2 concentrations. Melles et al. (2012) proposed that evidence for a collapsed Greenland Ice Sheet (Raymo and Mitrovica, 2012) and higher sea levels during MIS 11.c could allow for increased throughflow of warm water into the Arctic Ocean through the Denmark Strait, Fram Strait and Bering Strait, modulating warm conditions in the Russian Arctic.

Detailed changes in the local ecology of the lake and surrounding catchment observed in our records supports the labeling of MIS 11.c as a "super interglacial", as its diverse and abundant organism community is not matched in MIS 9, which demonstrates stronger summer insolation forcing (cf. Vogel et al, this volume). Additionally, reconstructions of global ice volume and bottom water temperatures from benthic foraminfera during this time period (Lisiecki and Raymo, 2005) display notable similarities, specifically a warmer and longer MIS 11.c as compared to MIS 9. Records from Lake Baikal indicate a particularly long MIS 11 (Prokopenko et al. 2010),

suggesting connections in the climate system over the Asian continent. Comparison of our biomarker record to the Lake Baikal biogenic silica record also shows a similar pattern and response to summer insolation. Additionally, in the Bering Sea, increased percentages of warm water diatom species, as well as decreased abundances of sea ice species, further indicate the ubiquitous warmth characteristic of this time period (Caissie, 2012).

While the temperature estimates made from the MBT/CBT index also record the stable, peak warmth of MIS 11, our reconstructions also reveal considerable variability absent in many records of global signals. For instance, temperature decreases noted at ~400 ka during MIS 11 and at ~325 ka during MIS 9 are not recorded in globally averaged records such as benthic foraminfera stacks. Initial comparisons of the 400 ka temperature drops with mid-latitude Atlantic Ocean records indicate the onset of MIS 11.b interstadial was demonstrated by a flux of ice rafted debris and a drop in δ^{18}O-based North Atlantic surface temperatures (Voelker et al., 2010). Additionally, alkenone ($U^{k'}_{37}$) sea surface temperatures in the North Atlantic (Lawrence et al., 2010) demonstrate a similar temperature decrease suggesting these events were not isolated to Lake El'gygytgyn. Evidence for early glacial inception from central Beringia suggests that at this time, the Arctic regions were beginning to cool with small changes in insolation (Huston et al., 1990; Brigham-Grette et al., 2001). Diatom assemblages in the Bering Sea also indicate cooler conditions, with increased percentages of sea ice species during this interval ~400 ka (Caissie, 2012). Although sea level was high (Raymo and Mitrovica, 2012) the presence of glacio-marine sediments overlain by till indicates the advance of glaciers coincident with the ~400 ka temperature drop (Huston et al., 1990). During the

mid-stage MIS 9 interstadial (9.b), changes in the Lake Baikal biogenic silica (Prokopenko, 2007) record can be roughly aligned with MBT/CBT temperature estimates as well (Figure 4). The response of the Lake El'gygytgyn record to these changes indicates the lake is sensitive to these global and regional changes, and thus is not solely recording local climate conditions.

2.7 Conclusions

Biomarker investigation allows for the reconstruction of not only temperatures based on the MBT/CBT paleothermometer, but also a semi-quantitative analysis of both terrestrial and aquatic productivity in the lake during MIS 11 and MIS 9. Results from this study corroborate the long duration of MIS 11 warmth of ~ 30 kyrs found in Lake Baikal by Prokopenko et al (2010) and in ice core records (EPICA Community Members, 2004). In concert with the long duration, the MIS 11 "super interglacial" interpretation by Melles et al. (2012) is supported by our results, with a diverse aquatic community indicated by high concentrations of all measured biomarkers. The overall record of MIS 9 and MIS 11 agrees with other records from various global locations as well, linking the Lake El'gygytgyn record to the global climate system. However, to further understand the ecological changes indicated by the biomarkers, future work must involve higher resolution sampling and analysis in addition to calibrations of the MBT/CBT paleothermometer so that absolute temperature may be reconstructed. Nonetheless, the results of this study indicate these biomarkers can provide critical information about paleo-ecological conditions, and shed light on how these climate changes are reflected in sensitive environments from Arctic regions.

2.8 Acknowledgements

Funding for this research was provided by the International Continental Scientific Drilling Program (ICDP), the U.S. National Science Foundation (NSF), the German Federal Ministry of Education and Research (BMBF), Alfred Wegener Institute (AWI) and GeoForschungsZentrum Potsdam (GFZ), the Russian Academy of Sciences Far East Branch (RAS FEB), the Russian Foundation for Basic Research (RFBR), and the Austrian Federal Ministry of Science and Research (BMWF). The Russian GLAD 800 drilling system was developed and operated by DOSECC Inc., the downhole logging was performed by the ICDP-OSG, and LacCore, at the University of Minnesota, handled core curation. Raw pollen data for was provided by Anatoly Lozhkin, NEISRI, and Patricia Anderson, University of Washington. We especially acknowledge NSF support for grant # EAR-0602471.

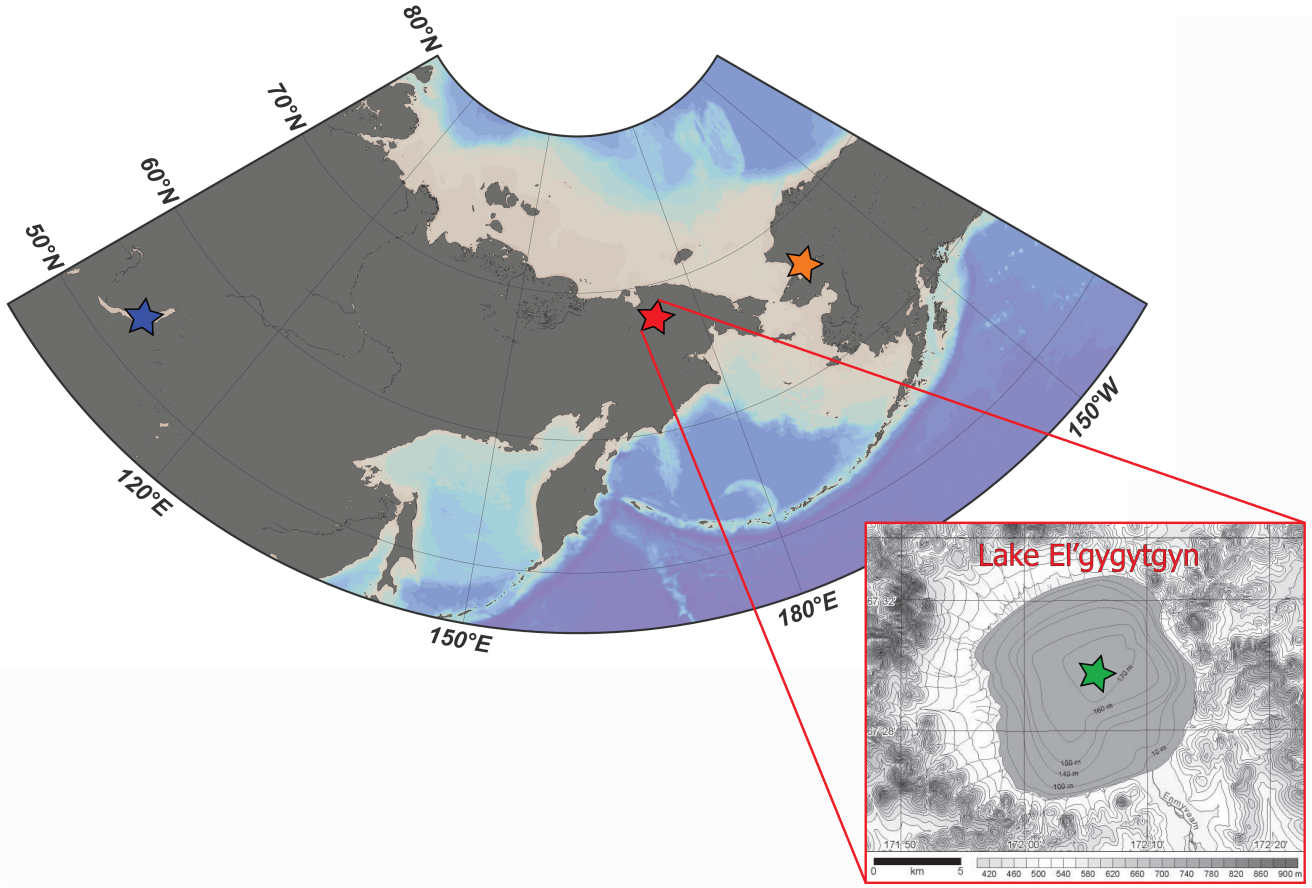

Figure 2.1: Location of Lake El'gygytgyn (red star) and corresponding ICDP 5011-1 drill site (green star, inset map) are indicated. Other points of interest to this study and in the region are Lake Baikal (yellow star) and the Baldwin Peninsula in Alaska (white star).

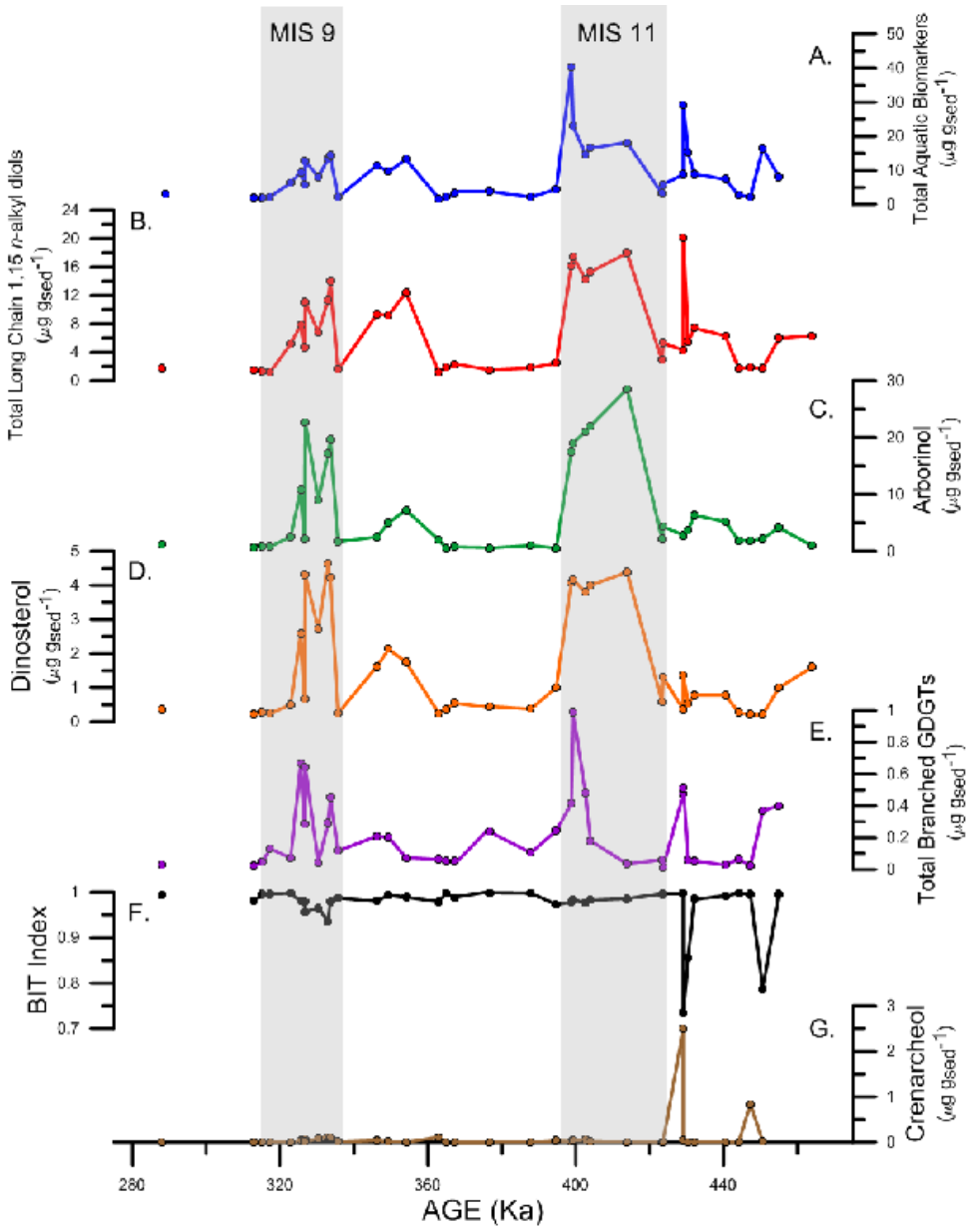

Figure 2.2: (A through G) Calculated and measured organic geochemical proxies for the period of 275 Ka to 475 Ka for: A) Total aquatic biomarkers, defined as the Σ [C_{17}] + [C_{19}] + [C_{21}] + [dinosterol] + [Σ long chain (C_{28},C_{30},C_{32}) *n*-alkyl diols]; B) Sum of long chain (C_{28},C_{30},C_{32}) 1, 15 *n*-alkyl diols; C) arborinol (µg g_{sed}^{-1}); D) dinosterol (µg g_{sed}^{-1}). E) Concentrations of total branched GDGTs (µg g_{sed}^{-1}); F) BIT index; G) crenarchaeol (µg g_{sed}^{-1}). Gray bars indicate the timing of MIS 9 and MIS 11 interglacial periods.

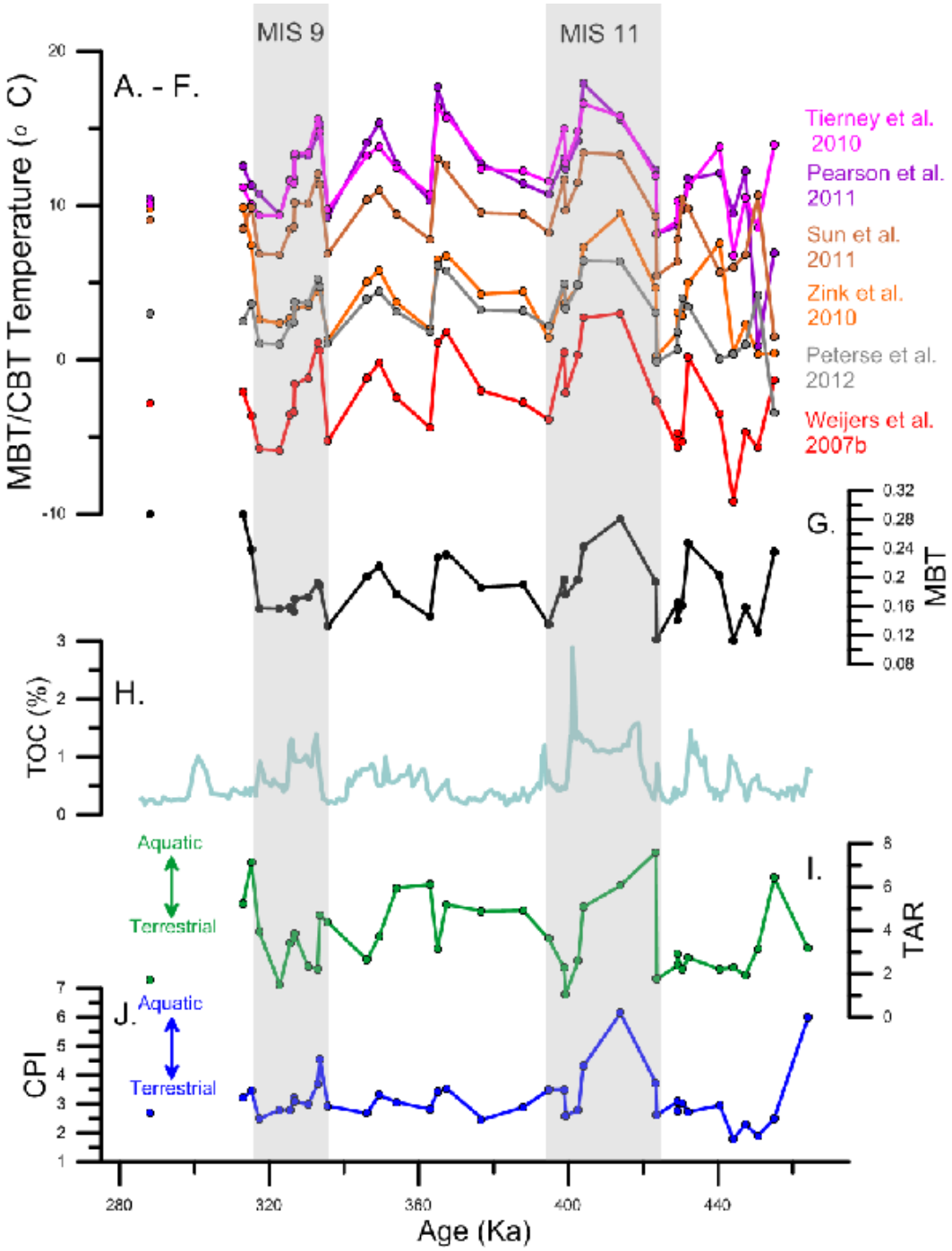

Figure 2.3 (A through J): MBT/CBT Temperature (°C) calculated from brGDGTs based on calibrations of A) Weijers et al., 2007b; B) Tierney et al., 2010; C) Pearson et al., 2011; D) Sun et al., 2011 E) Zink et al., 2010 and F) Peterse et al., 2012. G) MBT values; H) TOC data; I) TAR values, where the arrow indicates increased terrestrial input and J) CPI values, where the arrow indicates increased terrestrial input and/or OM preservation. Gray bars indicate the timing of MIS 9 and MIS 11 interglacial periods.

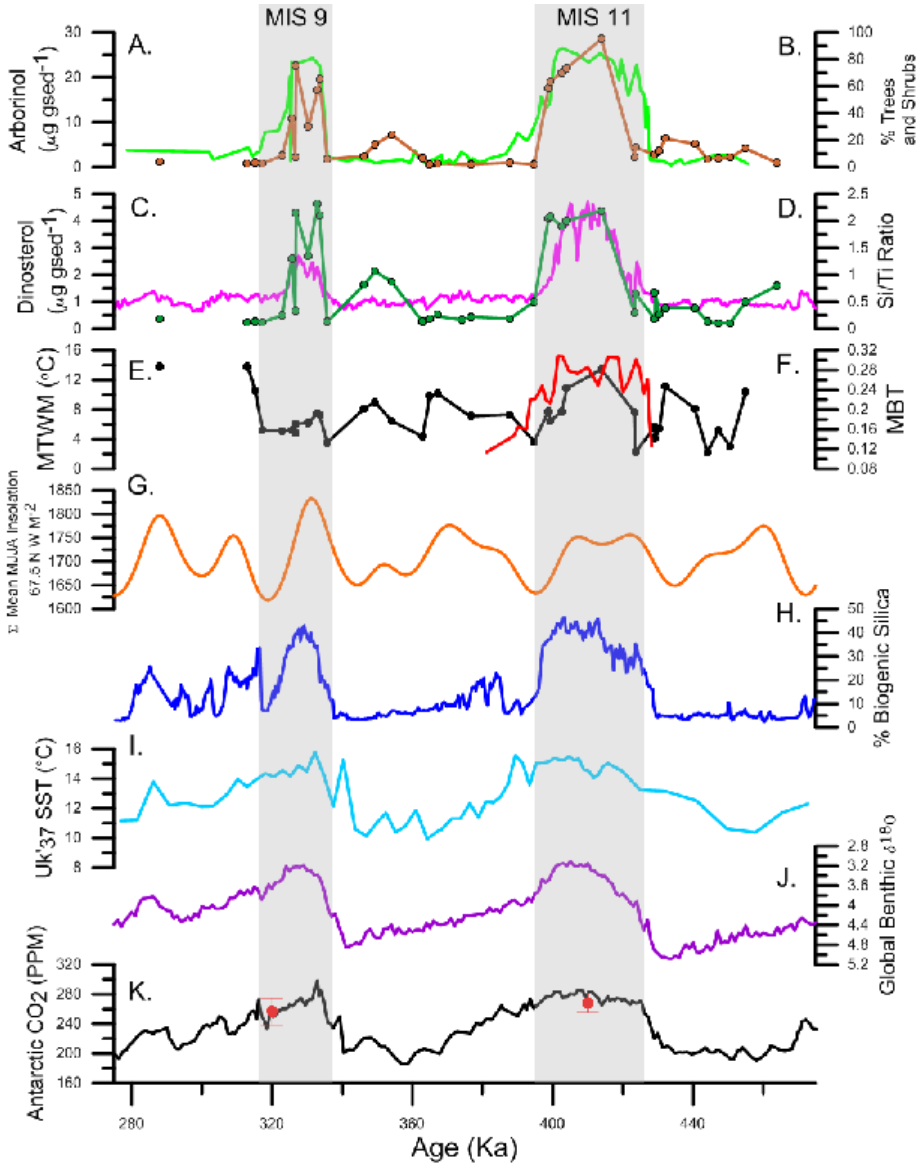

Figure 2.4 (A through K): A) Measured arborinol concentrations(μg g_{sed}^{-1}) (brown line and points)with B) measured tree pollen counts (green line) (from Lozhkin and Anderson, this volume, Lozhkin et al. 2007); C) dinosterol (μg g_{sed}^{-1}) (green points and line), compared with D) Si/Ti ratio (red line) from Melles et al. (2012); E) Calculated mean temperature of the warmest month (Melles et al., 2012) with F) calculated MBT ratio. G) The sum of Insolation from May, June, July and August (MJJA) from Laskar et al., (2004); H) The Lake Baikal biogenic silica record (Prokopenko et al., 2007); I) North Atlantic Sea Surface Temperature (SST) record from alkenones ($U^{K'}_{37}$) from Lawrence et al., (2010); J) Global benthic foraminifera δ ^{18}O stack from Lisiecki and Raymo, (2005) and K) Atmospheric CO_2 concentrations measured from the EPICA Antarctic Ice Core (EPICA Community Members, 2004), with red dots indicating average CO_2 concentrations for the MIS 9 and MIS 11 interglacial periods. Gray bars indicate the timing of MIS 9 and MIS 11 interglacial periods.

CHAPTER 3

EVIDENCE FOR ARCTIC CLIMATE CHANGE FROM SEDIMENTOLOGICAL AND COLOR REFLECTANCE SPECTROSCOPY INVESTIGATIONS THROUGH MIS 8 TO 12 FROM LAKE EL'GYGYGYTGYN, NE ARCTIC RUSSIA

3.1 Abstract

The sediment record from Lake El'gygytgyn provides essential information for understanding of how climate shifts drive lake and lake catchment process changes over time. Sedimentological results include the analysis of bulk mineralogy, clay mineralogy, iron oxide, and color measurements for the MIS 8 through MIS 12 interval. The hue color parameter, measured from high resolution core scans, suggests a link to global climate records, with green sediments reflective of cold intervals and red sediments indicative of warmer climate conditions. Validation of the color record was done in part by analyzing the clay mineralogy and the abundances of clay minerals. These data show that clay deposition dominates interglacial periods. Moreover the clay polytypes can be linked to bedrock weathering. Bulk mineralogy measurements allow for the reconstruction of synthetic color spectra which link mineralogy to sediment color. Overprinted on the mineralogical color signal is red color staining from iron oxide minerals, formed within the catchment during wet intervals when increasing amounts of eroded Fe – bearing silicate minerals are available for oxidation. If true, interpretation of the hue record then suggests hue is a proxy for wet/dry conditions within the lake, and when paired with the biomarker analysis shows significant warmer and wetter conditions during MIS 9 and 11. However, the hue record also demonstrates notable variability outside of these two interglacial periods, not recognized by other proxies, are not currently well understood. Overall, the multi-proxy results from this work can be further applied to the longer

temporal scale of the Lake El'gygytgyn sediment core, and potentially elucidate climate changes deeper into the Pleistocene, and even into the Pliocene portions of the sediment record.

3.2 Introduction

Marine Isotope Stage (MIS) 11 has been proposed as an analog to modern climate conditions, with orbital configurations similar to today and greenhouse gas concentrations at pre-industrial levels (Loutre and Berger, 2002; EPICA community members, 2004). Past studies indicate that MIS 11 was one of the warmest and longest interglacial periods of the past 3 Ma, with the characteristics of this "super" interglacial (Melles et al., 2012) period expressed globally in ice cores from Antarctica (EPICA Community Members, 2004), North Atlantic marine sediment core records (Lawrence et al., 2010), as well as in Asian lacustrine sedimentary records from Lake Baikal, which indicate a prolonged interglacial period of ~30 ky (Prokopenko et al, 2010). However, long terrestrial records from high latitude regions of the Asian continent are almost non-existent, yet can play a crucial role in understanding aspects of the Asian Arctic climate system and hemispheric teleconnections. The sediment record obtained from Lake El'gygytgyn in Far East Arctic Russia contains a continuous archive of climate variability since the middle Pliocene and permits critical analysis of the structure, and corresponding response of this Western Beringian lake system to changes during the MIS 11 "super" interglacial period.

The interval spanning MIS stages 8 through 12 is of particular interest to paleoclimatic studies because higher magnitude glacial-interglacial transitions, such as

the MIS 12 to MIS 11(Termination V) transition, were comparatively larger than previous glacial-interglacial transitions (EPICA community members, 2004). During the peak warmth of MIS 11, global sea levels are thought to have been significantly higher than other interglacials over the past 400,000 years possibly due to significant collapse of both the Greenland Ice sheet and the West Antarctic Ice Sheet (Raymo and Mitrovica, 2012). This interval, known as the Mid-Bruhnes transition, marks a period when the amplitude of interglacial – glacial variability increases after ~ 430 ka. Furthermore, past studies on Lake El'gygytgyn sediments by Melles et al. (2012), label MIS 11c as a "super" interglacial where lake sediments reflect high diatom and terrestrial plant productivity. Biomarker investigations by D'Anjou et al. (2013) demonstrated elevated terrestrial and aquatic productivity at Lake El'gygytgyn during the interglacial period, as well as during MIS 9. Additional work in this lake system confirms a shift towards warmer conditions during MIS 11 (Vogel et al., 2013), yet further analysis is needed to more completely understand interglacial – glacial changes and the effects on lake processes.

This study focuses on validating the use of color spectroscopy as a potential proxy for changes during the MIS 8 -12 interval. Color properties, measured by color reflectance spectroscopy include the hue color parameter (Nowaczyk et al., 2013), which are face value suggests a remarkable correspondence to global climate proxies such as global benthic foraminifera records (Lisiecki and Raymo, 2005, $r^2 = .58$, n = 239). The physical connection of the hue record to lake sedimentological dynamics and processes, however, was not yet understood, and past work involving mineralogy (Asikainen et al., 2007; Wennrich et al., 2013; Minyuk et al., 2012) did not cover the MIS 8 -12 time

interval where these “super-interglacial” sediment facies exist (Melles et al., 2012). By classifying the bulk and clay mineral components of the MIS 8 -12 sediment, which includes all three sediment facies (glacial, interglacial, and super-interglacial) found throughout the core, sediment mineralogy and components have been linked to rapid core scanning techniques. Building on past studies that have demonstrated how sediment mineralogy, clay minerals, and other properties can drive sediment color changes (Ortiz et al., 2009; Traschel et al., 2010), this study demonstrates the link between sediment mineralogy and color by directly comparing X-Ray diffraction (XRD) mineral analyses with investigations of the visible color spectral data and the calculated first derivative spectra (Barranco et al., 1989). In addition to XRD mineral analysis, further calibration tests to understand the relationships between organic content and Fe oxide minerals were also conducted in order to more completely explain the relationship between sediment facies and the color of the Lake El’gygytgyn sediments. By incorporating both mineralogical and color sensitivity tests, color reflectance spectroscopy is shown to validate sediment color as a proxy for environmental changes in Lake El’gygytgyn, and demonstrates the potential utility of this method for sedimentary systems.

3.3 Background and Setting

Lake El’gygytgyn is located on the Chukotka Peninsula in the Far East Russian Arctic (67°30’N, 172°5’E) (Figure 2). The catchment area sits within an impact structure formed at 3.58 +/- .04 Ma (Layer, 2000), with a rim-to-rim diameter of 18 km and a catchment area of approximately 293 km^2 (Nolan & Brigham-Grette, 2007). A network of 50 small streams carries surface runoff into the lake, and the Enmyvaam River serves

as the outlet to the Bering Sea (Nolan and Brigham-Grette, 2007). Lake El'gygytgyn is 12 km wide and 175 m deep with an approximate volume of 14.1 km^3 (Nolan and Brigham-Grette, 2007; Figure 1).

The bedrock geology of the surrounding catchment is dominated by a range of andesitic to rhyolitic rocks, consisting primarily of ignimbrites and tuffs of the Pykarvaam and Ergyvaam Formations (Bely and Raikevich., 1994) and to a lesser extent the Voronian Formation (ignimbrites and tuffs) and the Koekvun' formation (andesite-basalts, tuffs, and tuffaceous sands) (Minyuk et al., 2012; Bely and Raikevich., 1994; Bely and Belaya, 1998).

Modern precipitation levels are generally low, with cumulative precipitation from 2002 to 2007 ranging from 70 to 200 mm (Nolan, 2012). Strong winds also affect the El'gygytgyn area, with dominant directions out of the north or south and strongest winds in winter (Nolan and Brigham-Grette, 2007). The Lake El'gygytgyn region is located in an area of continuous permafrost, with erosion and sediment transport mechanisms dominated by weathering related to permafrost activity (Schwamborn et al., 2008). The modern vegetation around the lake can be characterized as arctic tundra consisting of lichen and herbaceous taxa (Lozhkin et al., 2007). Around the high-relief slopes of the catchment basin this flora is often limited and discontinuous. The closest modern day light conifer forests lie ~150 km SW of the lake, occurring as light conifer forest (Lozhkin et al., 2007).

3.4 Chronology

Sediment used by this study was taken from ICDP core 5011-1, extracted from Lake El'gygytgyn in spring 2009. Sixteen samples were taken at varying composite depth intervals between 13.9 m and 20.7 m composite with each sample representing ~250 to 500 years. The composite core record (Wennrich et al., 2013) was tuned from using tie points based on paleomagnetic investigations and the ages of oxygen isotope intervals from Lisiecki and Raymo (2005), which has a reported error of 4 ky for the 0-1 Ma interval. This work and synchronous tuning of 9 data sets between the paleomagnetic tie points was reported in Melles et al., (2012).

3.5 Color Proxies and Analysis

Color parameters, analyzed in previous studies (cf Debret et al., 2011) provided the framework for this research. Measurement of the different color components of the sediment facies from Lake El'gygytgyn and calculation of the hue color parameter are known to provide high resolution records of environmental changes from the region. This study utilizes the hue color parameter, calculated from the CIE (International Commission on Illumination) L*, a*, b* color parameter, and defined as Hue = atan2 (b*, a*). Color parameters were measured using color reflectance spectroscopy, which is a rapid and non-destructive core scanning technique. Other studies have used the CIE L*,a*, b* color parameters to track changes in sediment color due to changes in monsoon conditions in Asia (Ji et al., 2005), or to detect millennial scale changes in the North Atlantic ice rafted debris (Helmke et al., 2002), alongside a variety of other sedimentary applications in other ocean basins (Mix et al., 1992; Moy et al., 2002; Debret et al., 2006;

Deplazes et al., 2013). The hue color parameter is typically used as a measurable parameter from sediment cores, especially when used in conjunction with analysis of both the visible spectra (VIS) and first derivative spectra (FDS). The VIS and FDS color continuums provide a qualitative estimate of different minerals types within the sediment (Barranco et al., 1989), with distinctive patterns identified for iron hydroxide minerals (Deaton and Balsam, 1991, Debret et al., 2011) as well as organic material and pigment compounds (von Gunten et al., 2012; 2009). When paired with mineralogical analysis and identification, the visible and derivative spectra can link mineralogy and color visible measurements, such as hue, and allow for the rapid, non-destructive analysis of sediment core data (Trachsel et al., 2010, Ortiz et. al., 2009).

3.6 Methods and materials

3.6.1 Clay Methods

Sub sampling of the core material was carried out at the University of Cologne, in Germany. Facies specific samples were obtained, with ~5g samples taken for clay mineralogy every 1cm for selected intervals of the core.

Analysis of clay minerals utilized the filter transfer method (Moore and Reynolds, 1997), with samples processed and analyzed using a Phillips X-Ray diffractometer (CuKa radiation). Approximately 2 g of each sample were broken up and then sonicated for 30 minutes in 25 mL of water. Following sonication, each sample was centrifuged at 1500 rpm for 45 seconds. The supernatant was removed, and centrifuged and decanted once more in order to isolate the ~ 2 μm grain size fraction (clay minerals). Each supernatant was vacuum filtered through Millipore ® .22 μm filters and then transferred to a

petrographic microscope slide. Oriented slides were produced by carefully transferring the sediment collected on the filter paper to a cleaned slide; the sediment was then left to dry.

For XRD analysis, air dried samples were scanned from 2 to 35 2θ with a step size of 0.04 2θ, with 0.5 seconds for each step under a 1.541874 Å CuKa beam, and with a tension of 45 kV and an amperage of 40 (units). Following analysis o, each sample was then treated with an ethylene glycol-solvation to test for expandable layer clay minerals. Bulk weight percentages were calculated based on relative peak heights.

Additional analysis of clay polytypes was carried out, by measuring the 2 Theta angle range from 30 to 45 2θ. Diagnostic peaks for chlorite polytypes described in Brown and Bailey (1963) were used for polytype peak identification.

3.6.2 XRD Mineral Analysis

Analysis was performed using a programmed continuous scan from 5 to 65 2θ, a step size of .04 and a count time of 3 minutes with the same CuKa parameters discussed above. For both bulk minerals and clay minerals, identification was based off of multiple (5 or more) peaks, and weight percentages were calculated using peaks unique to individual minerals (Figure 3).

3.6.3 Grain Size Analysis

Grain size analyses were carried out using a Coulter LS 200 Laser particle size analyzer. Prior to processing, samples were treated with 10 ml 30% H_2O_2 to remove

organic content, 8 ml of .5M HNO_3 to remove diagenetic vivianite crystals, and 10 ml of 1M NaOH to remove biogenic silica for each ~ 1.5 g sample.

3.6.4 Color Reflectance Spectrophotometry

Raw color spectrum data were obtained by Nowaczyk et al. (2012) at AWI in Potsdam, Germany. A Gretagmacbeth Spectrolino™ spectrophotometer mounted on a specialized core scanning track obtained a full visible color spectrum from 380 to 720 nm at a physical resolution of 10 nms (36 bands), with a color measurement taken every 1mm. The instrument has a 4 mm diameter window, and utilizes a center weighted measurement technique. In addition to raw reflectance data, CIE L*, a*, b* values were obtained. The hue value was calculated from the a*, and b* values, and is defined by the equation Hue = atan2(b*,a*).

Processing of the raw color data was carried out with MatLab computer scripts written to calculate specific color parameters. First derivative spectra data (FDS Values; Barranco et al. 1989; Balsam and Deaton, 1991; Deaton and Balsam 2003) were also calculated from the raw visible spectra data.

In order to validate mineralogy and color continuums, mineral reflectance standards were downloaded from the USGS Spectral Library (Clark et al., 2007), and VIS and FDS continuums were calculated for each mineral. Based on mineralogical identifications performed by XRD analysis, USGS standards for the minerals quartz, albite, anorthite, orthoclase, as well as the clay minerals chlorite, illite and smectite were obtained (Figure 5). Based on bulk mineralogy results from XRD analysis, color continuums for sediments were constructed using standards and mineral abundances (Wt

%), and then compared to measured VIS and FDS components. Correlation (r) values for each of the 20 sediment samples were calculated in order to test whether the minerals present were the dominant source of the color signals.

3.6.5 Color Sensitivity Tests

Additional techniques were utilized to determine the relative effects of Fe-oxide and hydroxide minerals as well as organic content on sediment color reflectance measurements. Because Fe minerals are insensitive to the Cu radiation used by XRD analysis, other methods of mineral analysis were necessary. In order to test the color signal attributed to iron oxide minerals, additional investigations using scanning electron microscopy (SEM) and iron oxide digestions were performed.

For SEM analysis, thin sections obtained from all three described sediment facies were analyzed with a Zeiss EVO 50 SEM, with images and elemental (EDS) data obtained for a suite of mineral grains in each thin section.

For color sensitivity measurements, samples were filtered onto .2µm filter papers, with color measured on filtered wet sediments using a Konica Minolta 2600d spectrophotometer both prior to and following the iron digestion. Special care was taken to measure each sample before drying, as Balsam et al. (1998) found that progressively drying samples increases the brightness of sediment (higher reflectances) with time.

An iron oxide digestion protocol utilizing a citrate-bicarbonate-dithionite (CBD) treatment was applied to the sediment samples. ~2.5g of sediment was digested according to the treatment (Jackson, 1969) for all 20 sediment samples. To test the effect of iron oxide on sediment color, spectral measurements obtained following Fe-oxide digestion

were correlated to the artificially constructed color spectra, and a second set of correlation values calculated.

Similar to Fe digestion tests, classification of the effect of organic matter on color spectra was determined by obtaining color spectra and FDS values from selected intervals in the sediment core. Approximately 0.5 g of sediment was used to create filter samples, using a similar technique found in. Debret et al. (2006). Following reflectance measurements of the original smear slides, the sediment was treated with hydrogen peroxide (H_2O_2) to remove organic matter. Sediment samples were selected to encompass the range of TOC values found in the Lake El'gygytgyn sediments (.5 % to 3%). Color reflectance spectra produced from the two sets of analysis were then compared to determine the effect of organic matter on both visible and FDS spectra values.

3.7 Results

3.7.1 Mineralogy

The major mineral phases for all 20 samples consisted of quartz, potassium and plagioclase feldspar minerals, and chlorite and illite. Quartz and clay minerals comprised the majority of the sediment. Other minerals are known to be present, e.g. vivianite (Asikainen et al., 2007; Minyuk et al., 2013) yet vivianite was not detected. Quartz ranged from 37.3 % to 88.7 % while clay ranged from 0.2 % to 43.19% and feldspars (K-spar and plagioclase) comprised a relatively minor component of the sediment, ranging from 0.21 % to 9.9% and 3.6 % to 25.9 % respectively (Table 1). Relative changes in the feldspar minerals do not co-vary with quartz or clay, while changes in quartz and clay abundances are inversely related. Samples with high clay percentages and low quartz

abundances occur at 1335.1 cm, 1587.8 cm, 1813.8 cm, 1841.8 cm, and 2100.4 cm depth. For the clay rich intervals, the samples at 1587.7, 1813.8 and 1841.8 cm depth were found to correspond with the red laminated "super interglacial" Facies C, as in Melles et al. (2012), while the samples at 1335.1 cm and 2100.4 cm corresponded to the massive, Facies B (Table 1).

In addition to mineral identification by XRD, SEM analysis was used to determine the presence of the iron-titanium oxide ilmenite, as well as confirm the presence of quartz and feldspar minerals. For interglacial samples, many of the quartz and feldspar grains were found to be coated with Fe-oxide stains.

Three clay minerals were identified and quantified, with the largest component consisting of illite, followed by chlorite and smectite in terms of relative weight percent. While changes in the amount of total clay with respect to quartz occur on interglacial/glacial time scales, the relative percentages of clay minerals show a different trend. All three clay mineralogies do not fluctuate more than 10 % above or below the average values measured in the core section, with an average of 13.8% smectite, 59.3% illite, and 28.5% chlorite (Table 1).

Analysis of clay polytypes suggests chlorite polytypes described for the Lake El'gygytgyn sediments are of the IIb variety (Figure 3).

3.7.2 Grain Size Data

Grain size analyses revealed unique particle size differences between each of the three sediment facies. Overall, mean grain size varied between 5.8 and 16.6 μm (mean = 8.8), median sizes vary between 3.3 and 7.1 (mean = 4.1) μm and mode sizes range

between 2.3 and 13.6 µm (mean = 3.4). The distribution of Facies A sediments is skewed towards finer grain sizes (mean = 7.3, median = 3.4, mode = 2.6 µm), while Facies C contains more sediment falling into the coarser grain sizes (mean = 12.4, median = 4.2, mode = 2.7 µm). Facies B sediments fall in between Facies A and C, with a mean size of 8.3, median of 4.6, and mode of 3.8 µm. Variability in coarser (30 – 100 µm) sizes is most pronounced for the Facies C and some Facies B sediment samples.

3.7.3 Raw Color and VIS Data

The parameters of the CIE l*a*b* color parameters indicate changes in brightness (l*), variations between green (-a*) and red (+a*) as well as blue (-b*) and yellow (+b*). For the l* parameter, values vary between 4.32 and 65.77 % reflectance, with an average of 42.51. The a* parameter values vary between -6.18 and 2.81 with an average value of -1.41, while the b* parameter values range from -.97 to 18.94 with an average reflectance of 5.60, while the calculated hue value [Hue = atan2 (a*, b*)] has values which vary between 77.63 and 150.2 with an average hue of 107.59.

All of the color parameters except for the l* parameter suggest changes in sediment color through time. Changes in the l* parameter represent changes in the brightness of the sediment, which stays relatively stable at values of approximately 42 % reflectance. Color values in the red value range (lower values; red = 0°, 360°) at depths of ~1550cm to 1600 cm and 1800cm to 1900 cm, correspond to the red laminated facies (Facies C; Melles et al., 2012 Supplementary Materials) observed in the Lake El'gygytgyn core. At depths of 1300 to 1350 cm, 1600 – 1700 cm, and 1950 to 2100 cm~1550cm to 1600 cm and 1800cm to 1900 cm, the hue values are significantly higher

(Figure 4), corresponding to Facies A with green hue values (green = 180°). In between sections of red (Facies C) and green (Facies A) sediments, are the Facies B sediments, which vary in respective hue vales between red and green values. The a* and b* parameters follow similar trends as hue, although changes are more pronounced in the a* values with depth than with the corresponding b* values (Figure 4).

The inherent differences in hue values are reflected in varying VIS plots, as the structure of each spectrum for discrete depths downcore varies significantly, most notably in the ~550 nm to 730 nm range. The red, interglacial facies (Facies C) have a distinct structure with reflectance values highest in the ~600 nm to 700 nm band range, and a generally positive slope indicative of a positive relationship with increasing band length (Figure 5). On the other hand, the green, glacial facies (Facies A) also has a unique signature, characterized by a peak centered on the 550 nm band (Figure 5).

3.7.4 FDS Values

FDS values fluctuate most dramatically in the 550 nm portion of the spectrum, as well as from 600 to 700 nm. For the 550 nm spectral band, the most notable FDS changes occur at ~1550 cm to 1600 cm depth, ~1800 cm to ~1900 cm depth, as well as notable higher frequency fluctuations between ~1700 cm and 1800 cm depth. In the 600 – 700 nm range, changes in FDS values are not as dramatic as in the 550 nm band, but nonetheless fluctuate with depth. Highest values are found in the intervals at ~ 1550 cm to 1600 cm, 1700 to 1800 cm. The lowest values occur during the ~ 1700 to 1800 cm depth intervals, with low values from ~ 1950 cm, and from 2000 cm to 2050 cm composite depth (Figure 4).

The range of r values from the 20 sediment samples from correlations between measured and reconstructed FDS values range from .71 to .93, with the low correlation values found during the interglacial sediments (Facies B and C) and the higher values from the glacial (Facies A) sediments (Table 1; Figure 5).

3.7.5 Calibration Results – TOC and Fe Signal Analysis

Investigations into the effect of organic matter on the sediment reflectance parameters indicate significant changes between relatively organic rich sediments and sediments lacking in organic matter. The sediment sample with the lowest TOC percentage (0.29%) experienced the least change in the VIS spectrum, with a slight (1.8% reflectance) brightening of the sediments when organic matter was dissolved. In samples with higher values of TOC (.9% and higher), the VIS continuums show a larger brightening of the sediments, with average reflectance differences varying between 7.1% to 11.1% reflectance. Changes in the FDS continuums were also noted, with removal of organic material resulting in the accentuation of multiple peaks in the treated samples when compared with the original, organic rich sediment samples. Similar to the VIS measurements, minimal changes with the 0.29% TOC sample were noticed, while larger peak accentuations were observed for the TOC rich (0.9 to 2%) sediments (Figure 6).

Iron digestion sensitivity tests reveal for all facies a shift in the color spectrum towards the green portions (400 - 500nm) of the visible spectrum (Figure 6). Color measurements also demonstrate improved correlation coefficients (r values; Table 1) following the iron digestion techniques, with a smaller range of r values (0.88 to 0.96). Additionally, measured concentrations of digested Fe and Mn oxides range from 0.21 %

to 0.90 % by weight for Fe oxides, and 0.005 % to 0.027 % by weight for Mn oxides. Within facies, the mean concentrations of Fe for Facies A are .32 % (Std. deviation = 0.015%). For Facies B and C the mean concentrtaions measured were 0.44% (Std. deviation = 0.18%) and 0.29 % (Std. deviation = 0.14%) respectively (Table 1).

3.8 Discussion

The overall color signal demonstrates a remarkable correspondence to climate fluctuations, with clear color differences between sediments deposited during cold periods versus those deposited during warmer conditions. These color variations are not driven solely by large scale interglacial – glacial changes, although comparison to climate proxies records such as global benthic foraminifera stacks suggests these changes dominate the record (Lisiecki and Raymo, 2005, Figure 8). Notably, the hue parameter demonstrates variability on more rapid timescales than the changes between full interglacial and full glacial conditions (Figure 8), suggesting the hue parameter is recording a lake system that is sensitive to higher frequency shifts in past climate and environmental conditions.

3.9 Mineralogy

Analysis of the bulk mineralogy reveals shifts in relative inputs of the major minerals to the lake, as these shifts occur in conjunction with changes between interglacial and glacial conditions. Relative changes in the amounts of quartz and the input of clay minerals are the most notable. During glacial periods, quartz dominates the input to the lake, coupled with low amounts of clay minerals. Interglacial intervals, on the

other hand, show less quartz and more clay material deposited in the lake (Table 1). Higher inputs of clay are also not restricted to the defined interglacials MIS 9 and 11; rather, high clay input in samples corresponding with red hues outside of in Facies B suggest fluctuations in catchment processes. Interestingly, when compared to other available biological proxies such as biogenic silica, pollen counts (Melles et al., 2012; Vogel et al., 2012), or biomarkers (D'Anjou et al., 2013) from Lake El'gygytgyn during this time period, proxies for productivity fail to capture the variability demonstrated by the hue and mineral abundances (Figure 8). This suggests the hue parameter may capture the true variability of the physical and chemical catchment processes, and that catchment processes are sensitive to additional environmental changes not recorded in some other proxy records.

Unlike the glacial/interglacial variability of the bulk mineralogy, the relative amounts of the clay minerals chlorite, illite and smectite, remain relatively fixed throughout the MIS 8 -12 interval. Clay analyses show increases in the amount of clays but not a specific clay mineral, suggesting a catchment driven by mechanical weathering processes as opposed to the authigenic formation of clays in the catchment (Table 1). Analysis of chlorite polytypes supports mechanical weathering processes, as the IIB polytype was the only polytype identified for all sediment facies (Figure 3). The IIB polytype, which forms in metamorphic rocks (Hayes et al., 1970), demonstrates the detrital origin of the chlorite clay minerals, as authigenic chlorites would likely be of the Ia variety formed at lower temperatures (Walker, 1993). Thus, increases in the total amount of clay implies a wetter climate, with higher precipitation increasing the physical transport of clay material into the lake.

3.10 Color Sensitivity

Although mechanical weathering encapsulates the majority of weathering around the lake catchment, the variability in the color spectra not explained by XRD and reference mineral spectra implies additional sediment components and possible chemical weathering processes (Figure 5). Iron oxide minerals, especially the oxide mineral hematite, are known to stain sediments. Iron digestion tests demonstrate the presence of iron oxides in the sediments, and also the relative amount of color signals produced by iron oxide staining (Figure 6). For Facies B sediments, removal of iron oxides results in green color signals resembling sediments from the glacial Facies A. Calculated correlation values for all facies improve significantly when FDS continuums from mineral abundance reconstructions are compared to those measured following the iron digestion (Table 1), demonstrating that bulk mineralogy contributes a significant background color signal. When increases in the amount of iron oxide formation in the catchment occurs, these oxides contribute a red color signal in addition to the background mineral colors, which ultimately stain the sediments red and are reflected in the low hue values observed during both Facies B and C.

When the iron digestion tests are applied to Facies C, however, notable reflections in the red portion of the spectrum still exist, suggesting the red hues from Facies C are driven by both the iron oxide and TOC signals. Results from color sensitivity tests elucidate the relative effects of organic matter and iron oxide minerals on color spectra. Organic matter inputs, which can be approximated by TOC, brighten sediment color when removed, especially in the red (600-700 nm) wavelengths of the visible color spectrum (Figure 6). Low TOC values (< 0.5%) correspond to glacial sediments and

Facies A, and these sediments exhibited the smallest measured color change from TOC sensitivity tests. In sediments where TOC percentages are highest (up to 2%) corresponding to the "super interglacial" stages (Melles et al., 2012), the most sediment brightening with the removal of organic content occurs while also contributing a color signal in the red portions of the visible spectrum. Previous color investigations have shown that high TOC content drives sediment color changes in the visible spectrum (Debret et al., 2011), and various pigments from chlorophylls and carotenoid compounds also have visible reflections in the red portion of the visible spectrum (Rein and Sirocko, 2002; Wolfe et al., 2006). These results elucidate key differences between the red sediments between Facies C and Facies B; that is the red hues in Facies B are derived from iron oxides while red hues in Facies C are both iron oxide and organic matter driven. While hue values may suggest similar processes occur during the deposition of both Facies C and B, analysis of the FDS and visible color spectra reveal the weathering differences which define Facies C as "super interglacial" periods.

3.11 Iron Digestion Solution Analysis

Coupled with analysis of the color signal from iron oxide removal, analysis of the Fe and Mn ions present in the digested solution supports mechanical weathering processes sourced from the lake catchment. The concentrations measured demonstrate similar, low concentrations of Fe for Facies A sediments, while the measurements for Facies B and C exhibit a wide range of concentrations and cannot be differentiated from one another. Both iron oxides and manganese oxides are ubiquitous in soils (Jackson 1969; Post, 1999), and the erosion, transport, and deposition of these oxides into lake

sediments drives the hue color parameter. For Facies A, the low measured Fe and Mn content corresponds with the greenish/grey sediment colors, supporting the color analysis which points to a lack of available material for oxidation in the catchment during drier periods.

In contrast, the Fe and Mn concentrations for Facies B and C sediments demonstrate higher variability than the Facies A sediments. For some Facies B and C sediments, high amounts of clay and red hue values are associated with relatively high abundances of iron oxide material, while other samples demonstrate low measured iron oxide abundances despite red hue values. For the samples with red hues and high concentrations of iron oxides, the red sediment color can be directly linked to iron oxide staining, and an increase in physical weathering and transport. The processes affecting samples with lower oxide abundances but with red hues, however, can be linked with periods of high TOC in some cases (3 of the Facies C samples, and Facies B at 1335.1 cm depth), indicative of higher rates of organic deposition and/or preservation. As discussed above, organic matter contributes a red color signal, and for these sediment samples, particularly the Facies C sediments, the red hues are generated from a mix of iron oxides and organic inputs.

Samples with both low iron oxide abundances and low TOC suggest additional processes; interpretations by Melles et al. (2012) suggest periods of oxygen depletion within the water column during the deposition of both Facies A and Facies C. Analysis of the Mn and Fe abundances based on the digestion solution measurements and the calculated Mn/Fe ratio, however, do not support this hypothesis, as none of the three Facies demonstrate consistent ratio values. Instead, the measured abundances and the

calculated Mn/Fe ratio implies variability in the preservation of both iron and manganese oxides in the sediment, and that suboxic conditions may have persisted at different times and to varying degrees within the water column.

3.12 Interglacial/Glacial Period Variability

The suite of analyses examined in this study provides insights into relationships between past environmental conditions and sediment color. Glacial period sediments (Facies A) are characterized by a unique color signature, with higher hue values indicative of a green/grey color. The overall green color of the glacial sediments reflects a largely detrital mineral signal, with total clay, TOC values, and digested iron oxide concentrations all low during these times. Such a color signal dominated by mineral input suggests that processes such as chemical weathering were almost non-existent during glacial intervals, indicative of a cold and dry lake catchment. Mechanical weathering processes typical of cold environments were most likely active but still limited, as demonstrated by the lack of variations in clay minerals as well as chlorite polytypes and the Fe and Mn digestion solution data. Drier conditions would limit the production of physically weathered material Fe-bearing silicate minerals, and therefore limit iron oxide input into the lake, coloring the sediments the distinctive green/grey hue.

The red color measured in many Facies B samples corresponds with the presence of Fe-oxides/hydroxides during wetter intervals. The relationship between Fe oxides such as hematite is well known in both soils (Torrent et al., 1983) and in sediments (Balsam and Deaton, 1991), and it must be noted that small amounts of iron oxide abundances (< 0.5%) can drive sediment color changes (Balsam and Deaton, 1991). For this lake

system, the color signals represented by iron oxides are overprinted on the background mineralogical color signals, represented in the green Facies A. Thus the presence of increased Fe-oxides implies a slightly greater degree of chemical weathering around the lake catchment, as enhanced physical erosion as a result of wetter environmental conditions would increase the amounts of Fe-bearing silicates available for oxidation, and their ultimate deposition in the lake sediments. Interestingly, periods of enhanced iron oxide deposition do not necessary occur in conjunction with interglacial periods, suggesting wet intervals not coincident with interglacial/glacial variability.

Facies C sediments, while demonstrating red hue values as well, do not share the same sedimentary components as their Facies B counterparts. As the color signal from organic inputs also contributes a red color, the Facies C sediments can be linked to climate conditions that were both warm and wet, as demonstrated from VIS and FDS continuums. These facies occur in MIS 9 and 11 and are interpreted as "super interglacial" intervals (Melles et al., 2012), an interpretation supported by previous pollen reconstructions (Lozhkin et al., 2013) and biomarker data (D'Anjou et al., 2013). These differences then set the red Facies C sediments apart from the red Facies B sediments in terms of lake processes, and allow for paleoclimate interpretations of the hue record.

The hue record overall can be interpreted to represent the gradational changes of the lake from relatively dry to relatively wet conditions. Enhanced moisture around the lake during these periods produced more material for chemical weathering, which is represented by red iron oxide staining ultimately overprinted on a glacial background mineral color signal. It must be noted, however, that although similar red hues for Facies B and C exist, the "super interglacial" periods during MIS 9 and 11 represent climatic

intervals that were relatively warm and wet, while red Facies B sediments reflect only enhanced moisture. Based on this assessment, interesting wet periods stand out in the hue record, most notably during MIS 6, 8, 10 and 12. While some suggested moisture intervals, like those in MIS 8, can be linked to global climate shifts apparent in global records, enhanced moisture events such as those in MIS 10 and 12 do not appear at a hemispheric scale. Notably, a cold yet moist MIS 6 in Mediterranean Sea region (Bard et al., 2006) as well as African monsoon enhancement have been recorded (Tisserand et al., 2009), and may be seemingly recorded in the Lake El'gygytgyn hue record. These color measurements from the entire length of the ICDP 5011-1 core can then potentially provide continuous, climatic information for glacial/interglacial periods not yet understood in the terrestrial Arctic setting.

3.13 Conclusions

This study demonstrates overall the strong relationship between sediment mineralogy and other sedimentary components on the ultimate sediment color, measured by high resolution core scans. The use of sediment color, and specifically the hue color parameter, can then be used as a proxy for processes occurring within the Lake El'gygytgyn processes. The color signal is dominated by clastic inputs, demonstrated by measuring bulk mineralogy and pairing these data with color spectra reconstructions. Color sensitivity tests show the importance of both organic material and iron oxide minerals on sediment color as well, with these minor sedimentary components overprinting their color signal over those of the background mineral content. The fluctuating concentrations of various sedimentary components are driven by the dominant mechanical erosion and physical transport of sediment into the lake basin, with physical

processes demonstrated by clay mineral analysis. Interpretation of the hue color proxy suggests that there is an intensification of physical weathering processes occuring during wetter periods, driving more clastic input as well as increasing iron oxide formation, which in turn drives the observed color changes from green sediment during cold, dry glacial intervals to red sediments during warmer and wetter interglacial intervals. Overall, the validation of the hue color record provides insight into climate fluctuations for the MIS 8 through MIS 12 interval, and the techniques discussed in this study can be used to calibrate and analyze future sediment records where high resolution core scanning techniques are applicable.

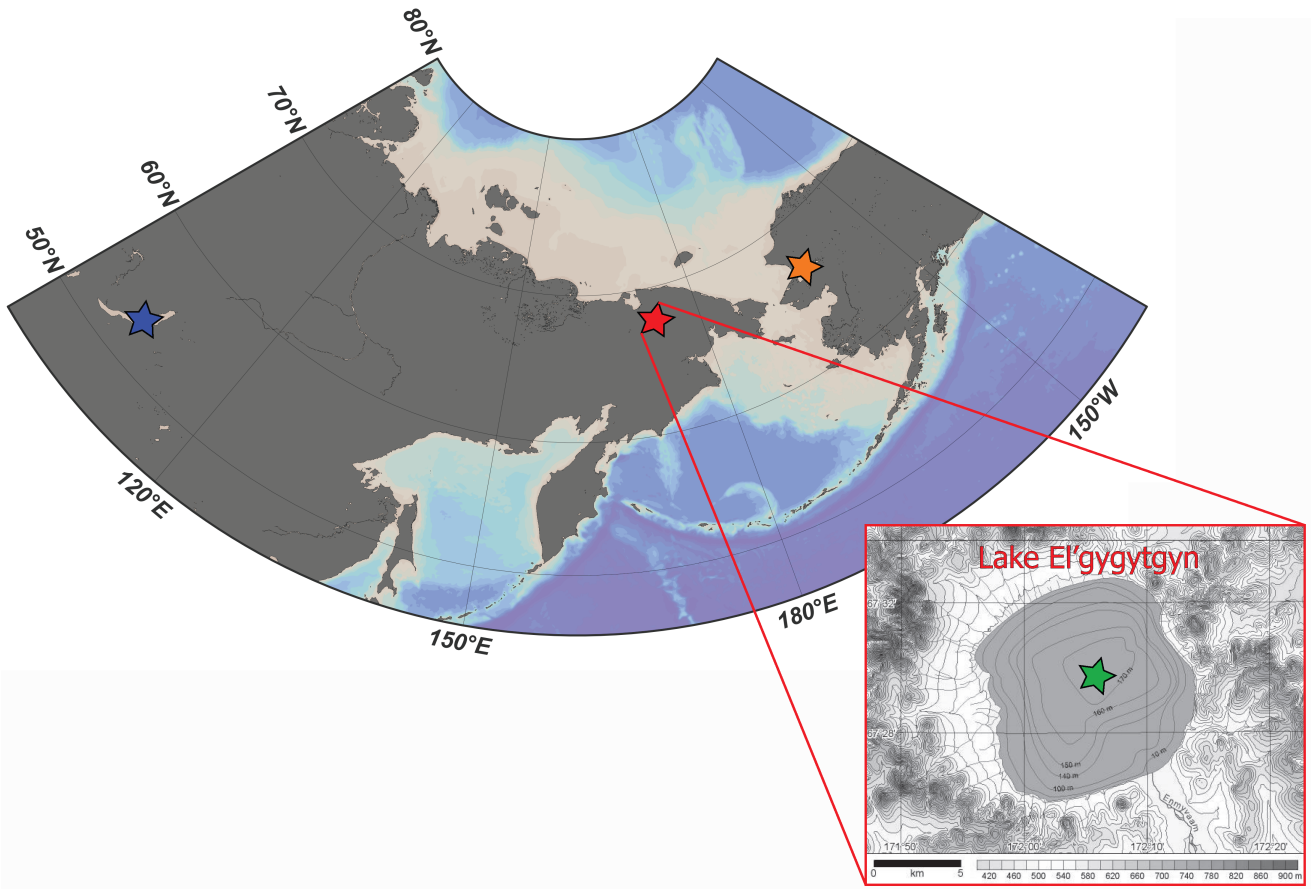

Figure 3.1: Location figure demonstrating the location of the lake (red star), as well as an inset map marked with the location of the ICDP core 5011-1 (green star).

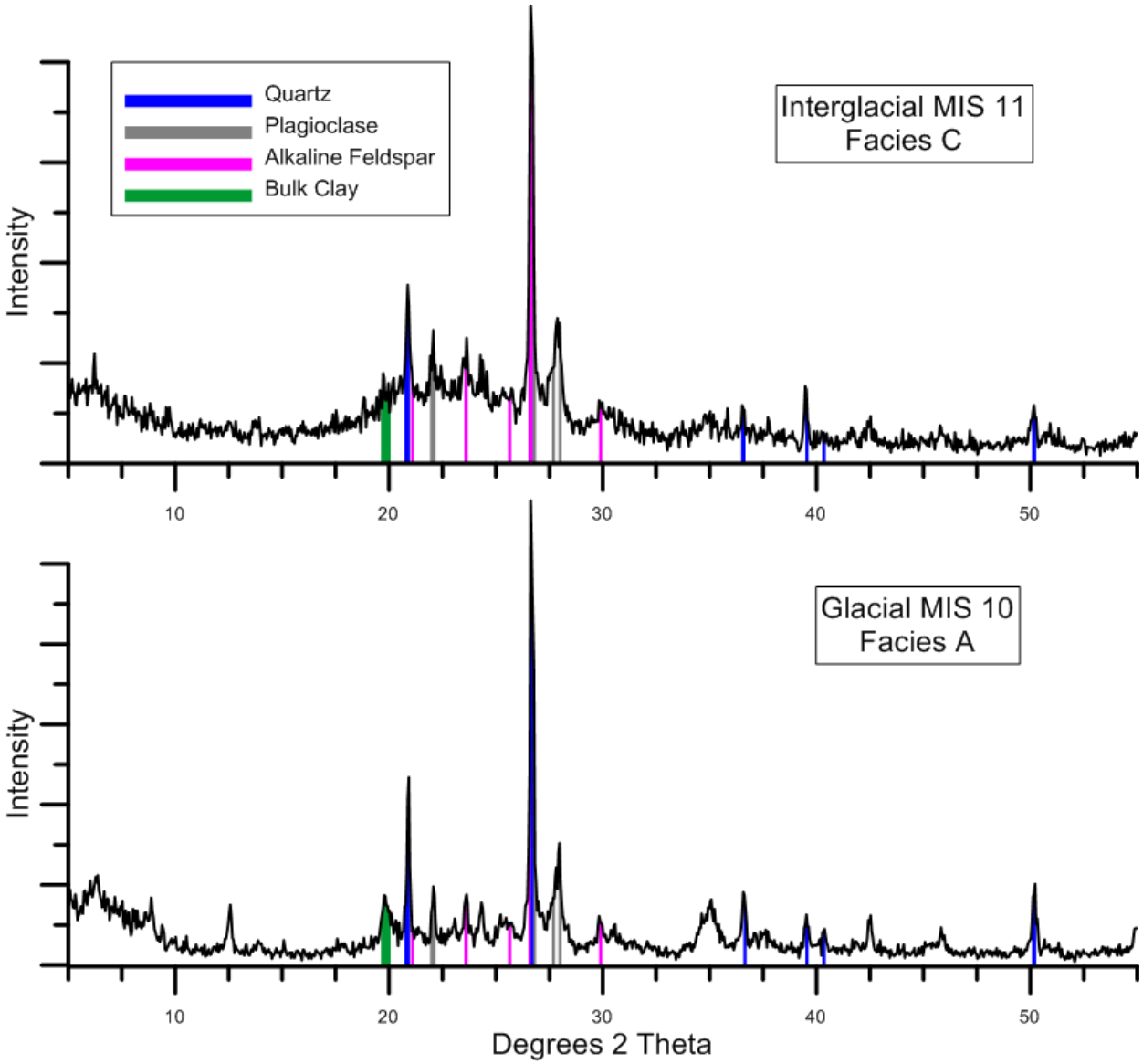

Figure 3.2: Representative bulk XRD diffractograms for both an interglacial and glacial samples. Peaks used for major mineral identification are colored for quartz (blue), plagioclase (grey), alkaline feldpsars (magenta), and the shared bulk clay peak (green).

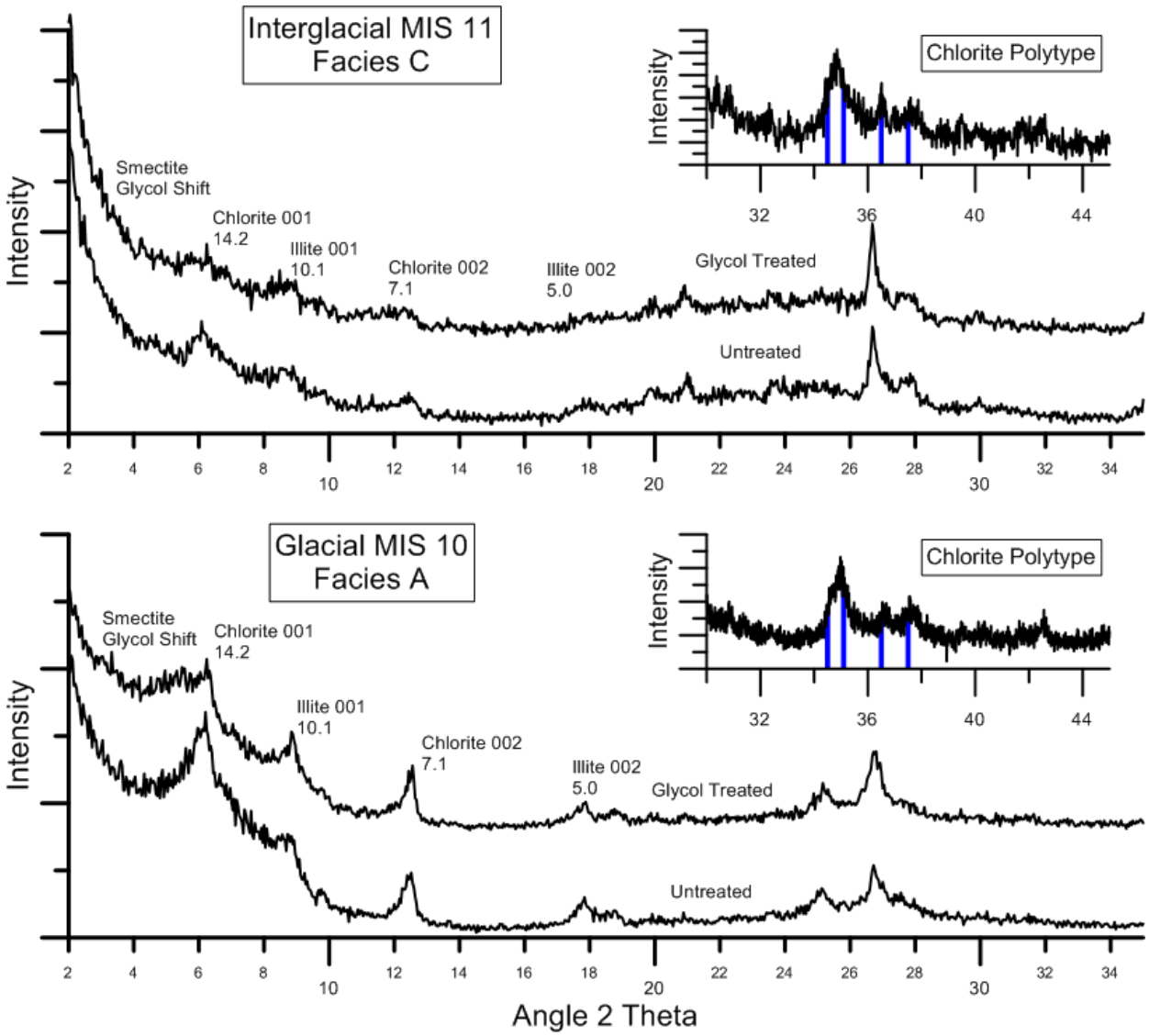

Figure 3.3: Representative clay diffractograms for an interglacial and glacial sediment sample. Peaks used for identification are marked (d-spacings in angstroms). The insets demonstrate the chlorite IIB polytype peaks (blue) for both representative samples.

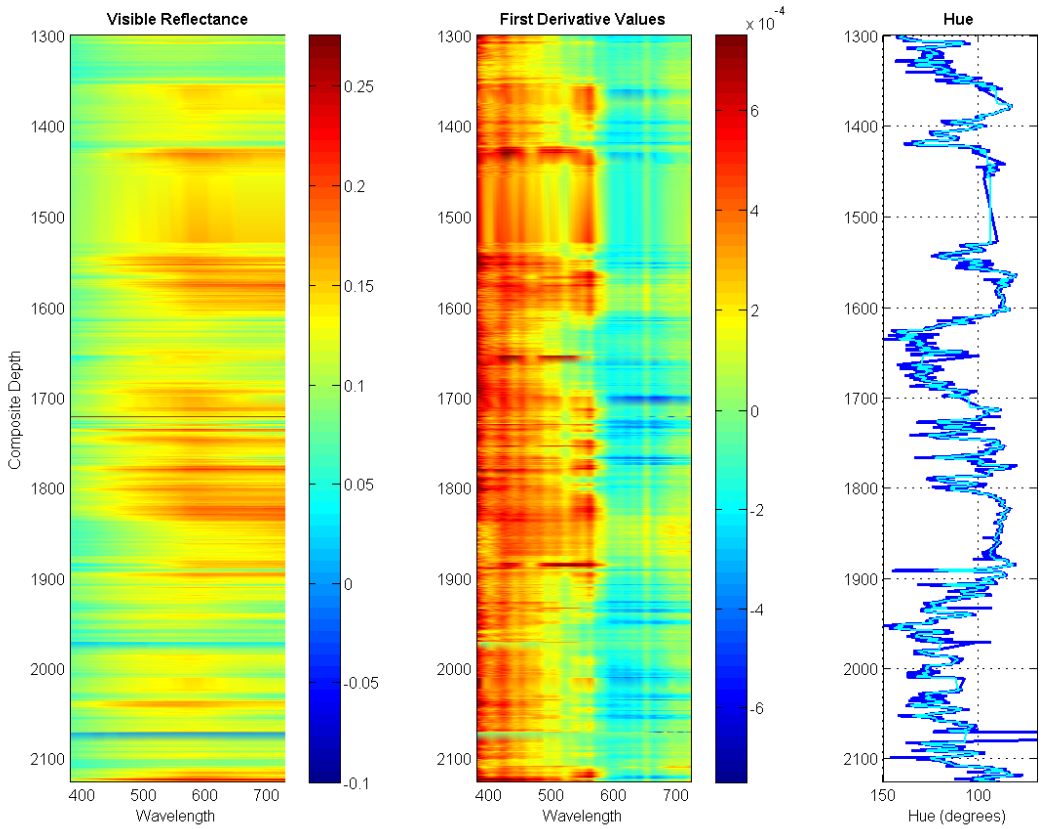

Figure 3.4: Surface plots colored to represent the variability of both VIS (left) and FDS (middle). Both the VIS and FDS can be linked to the hue color parameter (right), with higher VIS values in the red (600-700nm) area correlated to lower (red) hue values. Note the variability in the FDS values in the 550 nm range, as studies link variations in the 550 nm wavelength to iron oxide content (Deaton and Balsam, 1991; Debret et al., 2011).

Depth	Facies	% Clay	% Qtz	Calculated FDS vs. Measured FDS	Calculated FDS vs. Fe Digested FDS	Hue	Fe Solution Data (wt %)	Mn Solution Data (wt %)
1379.5	**A**	7.40	86.25	0.76	0.95	115.95	0.302	0.014
1648.4	**A**	10.04	83.88	0.91	0.94	113.62	0.332	0.008
2100.4	**A**	35.43	44.89	0.85	0.94	118.06	0.326	0.017
1294.1	**B**	6.02	88.34	0.93	0.91	133.23	0.431	0.011
1335.1	**B**	40.47	44.20	0.90	0.95	84.381	0.868	0.027
1530	**B**	12.49	76.72	0.82	0.95	94.312	0.435	0.012
1577.7	**B**	8.15	63.97	0.78	0.90	90.456	0.523	0.017
1670	**B**	8.49	83.62	0.91	0.95	126.43	0.265	0.008
1712.1	**B**	16.35	69.54	0.85	0.96	90.994	0.266	0.013
1936.3	**B**	0.19	81.45	0.93	0.93	129.4	0.491	0.023
1988.6	**B**	17.15	75.07	0.89	0.94	114.18	0.450	0.010
2152.5	**B**	5.42	88.76	0.71	0.90	87.301	0.241	0.005
2175	**B**	0.87	76.97	0.74	0.91	87.667	0.436	0.019
1587.8	**C**	37.86	38.56	0.83	0.92	87.779	0.218	0.008
1813.8	**C**	31.94	50.21	0.88	0.88	91.92	0.201	0.012
1841.8	**C**	43.19	37.35	0.80	0.92	89.15	0.463	0.035

Table 3.1: Breakdown of various data measurements by the facies description of Melles et al. (2012). See text for detailed descriptions of various measured parameters.

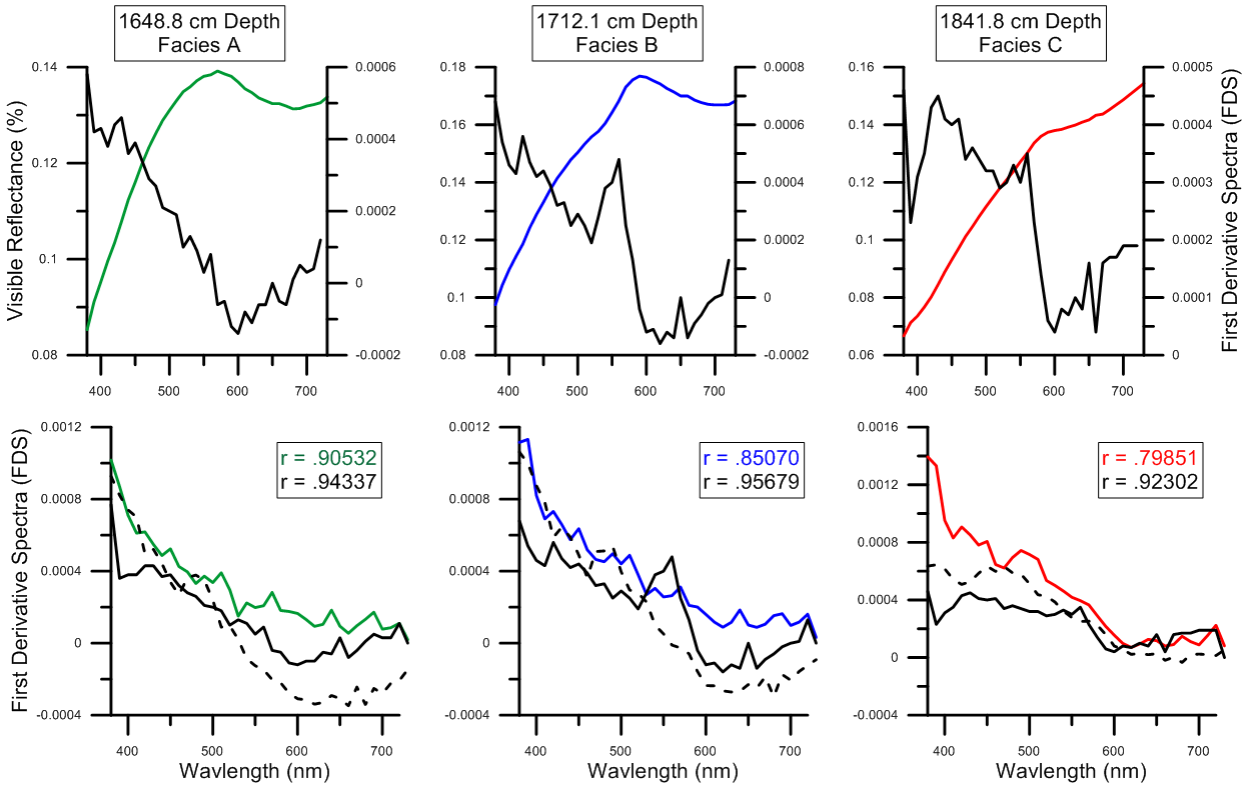

Figure 3.5: The three top plots demonstrate VIS (colored) and FDS (black) plots for selected samples representing the three sediment facies. The three bottom plots show calculated FDS values for the core measurements (black), the reconstructed FDS based on mineralogy (colored) and FDS calculated post iron digestion (dashed black). R values compare the correlations between measured FDS and reconstructed (colored r values), as well as the correlations between reconstructed and post iron digestion analysis (black r values).

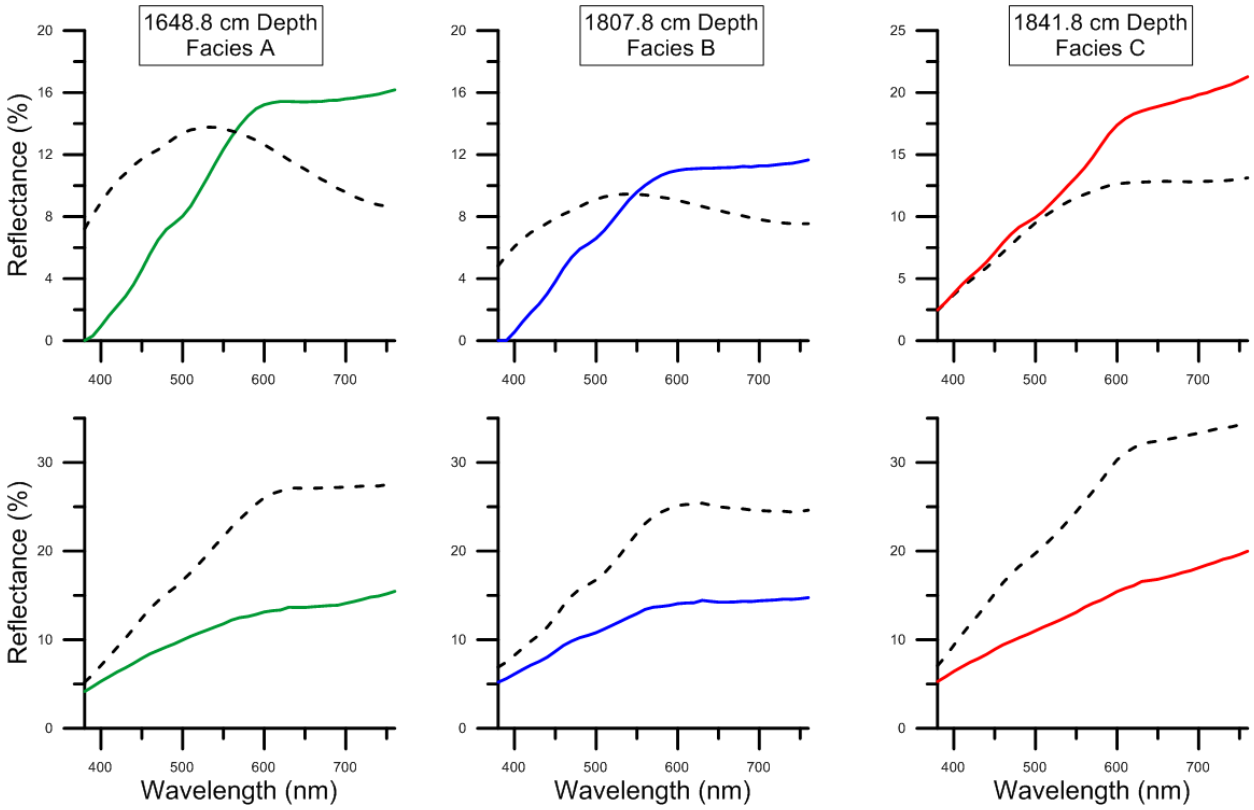

Figure 3.6: Top plots demonstrate the measure color VIS continuums before (colored plots) and after (dashed black) iron digestion tests for representative facies samples. Note how the spectra shifts to centering on the green (~500nm) wavelengths. Bottom plots show before (colored plots) and after (black dashed) TOC removal by H_2O_2 treatment. Notable increases in reflectance are observed post removal of organic content.

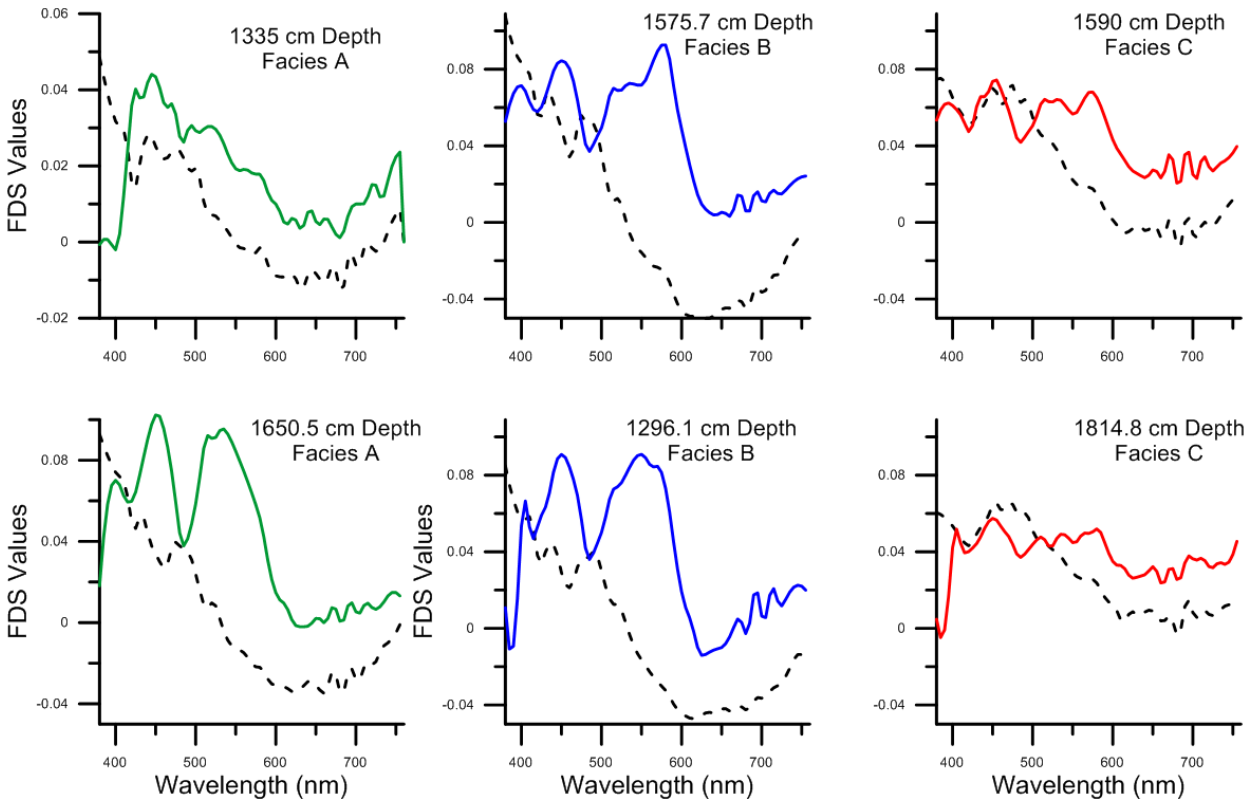

Figure 3.7: Calculated FDS values for iron digestion experiment for representative facies, before (colored) and after (dashed black) iron oxide removal. Note how peaks at 450 nm and 550 nm disappear post removal of iron oxides, similar to results from prior studies of iron oxides and sediment color (Deaton and Balsam, 1991; Debret et al., 2011).

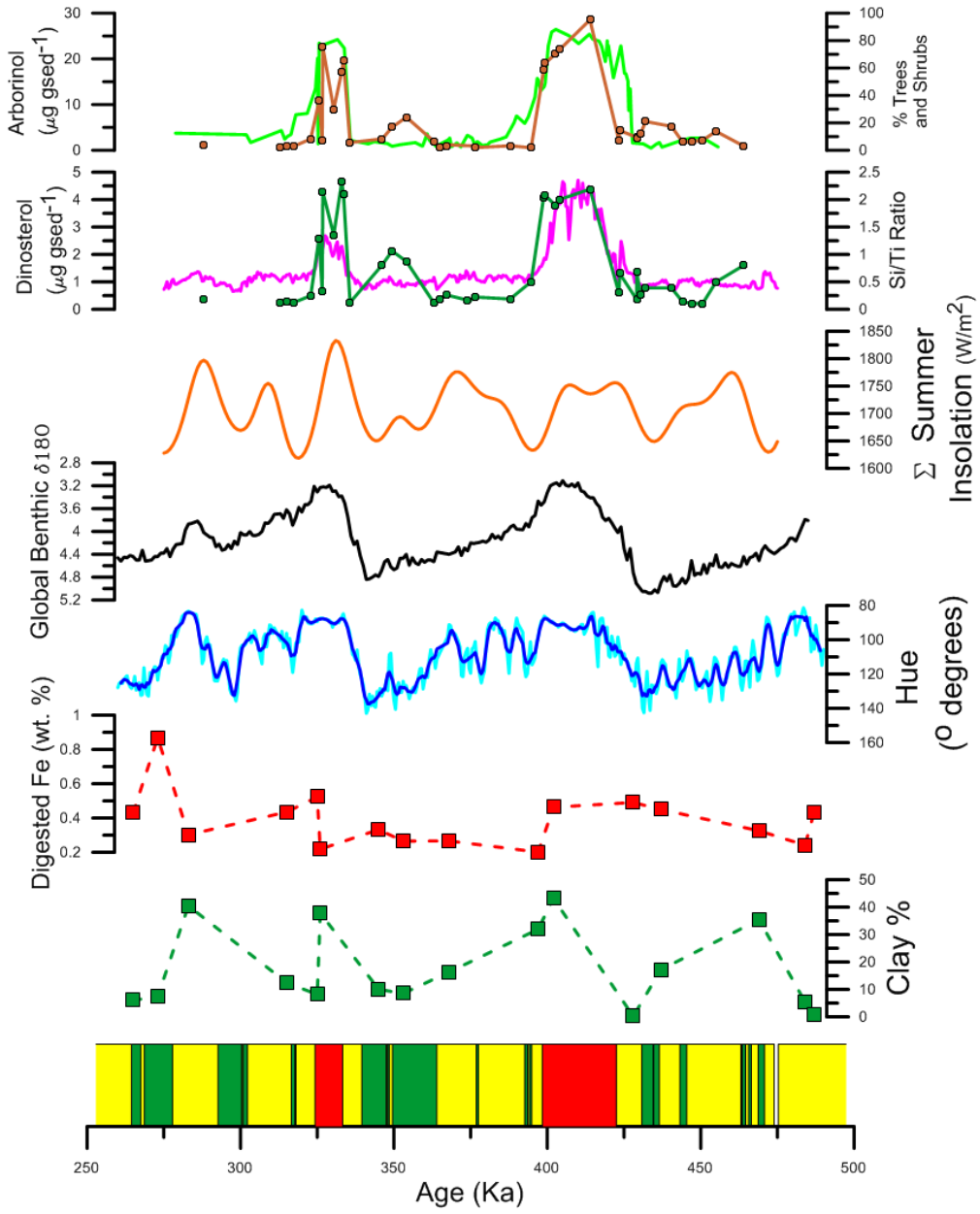

Figure 3.8: Comparison of the biomarker records from D'anjou et al., 2013, with concentrations of arborinol and dinosterol, as well as pollen counts (Lozhkin et al., 2013), and the Si/Ti ratio (proxy for diatom production, Melles et al., 2012) with the sum of summer insolation at 65 o N (Laskar et al., 2004) the global benthic $\delta^{18}O$ stack (Lisiecki and Raymo, 2005), the hue color parameter, digested Fe-oxide concentrations, clay percent (this study), and the Facies interpretations by Melles et al., 2012.

CHAPTER 4

THE FURTHER RESEARCH POTENTIAL FOR THE LAKE EL'GYGYTGYN RECORD

4.1 Abstract

Further investigations building on both the biogeochemical analyses and the understanding of chemical and physical lake processes can be undertaken in the future to forward the knowledge gained from interpreting the Lake El'gygytgyn sediment record. With the unprecedented length and continuity of this sediment record, future investigations are indeed critical for placing both past and future climate changes in context.

4.2 Introduction

Investigations of the Lake El'gygytgyn sediment record, based on the findings of this work, will progress the understanding of the lake's response to climate changes, as well as document regional and global climate changes through time. Biomarker records and proxies can be utilized to investigate intervals of particular interest. High resolution work involving not only the MIS 8 through MIS 12 interval, but also MIS 31 and other "super interglacials" will contribute to understanding periods of global interest and significance. Additional work with the color record can be applied to other intervals of interest as well, with future validation critical for linking color to sediment components for the entire core. Furthermore, the sediment color record from the deeper Pliocene sections has not yet been investigated, providing an opportunity for the future development of the Lake El'gygytygn record.

4.3 Biomarkers

The biogeochemical investigations conducted for MIS 9 and 11 were among the first for the terrestrial Lake El'gygytgyn record older than the last interglacial period, and provide the necessary background for future investigations. Specifically, future biomarker work can be shifted to focus towards understanding other time periods and other compounds in the lake, and potentially demonstrate the ability of specific biological proxies to capture climate parameters including mean annual temperatures. The application of the rapidly growing biomarker literature, bridging both the marine and terrestrial realms, suggests future studies from Lake El'gygytgyn will provide a further understanding of how the lake ecosystem responds to climate changes, and contribute towards the use of biomarkers as recorders of climate change.

The results from Chapter II demonstrate the sensitivity of multiple organic compounds, and their ability to capture shifts in climate parameters for the Russian Arctic region. The biomarker record suggests not only the long duration of the MIS 11 interglacial period, but also the intensified warmth of the subsequent interglacial period MIS 9. What is poorly understood, however, is how quickly the lake system can respond to rapid and dynamic climate shifts not captured by the low resolution sampling of this study. This work demonstrates the need to focus on measuring changes in biomarker concentrations at a finer scale, perhaps to detect subtle climate changes suggested by high resolution core scanning techniques. Using high resolution biomarker analysis, periods coincident with Northern Hemisphere ice sheet inception around 2.8 Ma (Brigham-Grette et al., 2013), as well as other "super interglacial" periods (Melles et al., 2012) can be

further understood. The multiple proxies investigated capture different aspects of biological productivity in the lake, and when paired with other measured proxies provide a more complete picture of the biological response interglacial/glacial cycles and climate shifts.

Additional field work is needed in the future to collect modern samples for validation and calibration of the branched GDGT measurements. This will have a large impact on the development of the MBT/CBT proxy, with implications for both the Lake El'gygytgyn record and the additional development of the proxy itself. Currently, multiple calibration sets exist for the MBT/CBT temperature estimate proxy, many of which are global (Weijers et al., 2007; Pearson et al, 2011; Peterse et al., 2012) while others are specific only for regions such as Africa (Tierney et al., 2010) or Asia (Sun et al., 2011). These multiple calibrations suggest similar responses of the branched GDGTs to annual temperature changes, but existing global and regional calibrations are unlikely to accurately capture local Lake El'gygytgyn variations in temperatures across the Russian Arctic. Additional field work involving the sampling of soils and additional surface sediment cores from the lake catchment area, when paired with modern meteorological data, could result in the calibration for the MBT/CBT. The producing organism is thought to exist in soils (Weijers et al., 2007), and sampling of modern soils is critical for understanding these processes. However, investigations into MBT/CBT sources potential show that these organisms may also exist in-situ in the water column, which can be understood by deploying sediment traps at multiple water depths along with surround soil and surface sediment samples. Other temperature proxies that are based on molecular fossils also exist, such as the diol temperature index based off long chained *n*-

alkyl diols (Versteegh et al., 1997; Rampen, 2012). These proxies can also be potentially measured and compared to the results from a calculated MBT/CBT proxy to further development biological temperature proxies. Given the high inter-calibration variability between the separate calibration studies, lake calibration allows for a better understanding of temperature variations at Lake El'gygytgyn at times during the past, when paired with high resolution measurements.

4.4 Sedimentary Pigments

Previous work by multiple authors has investigated the presence of sedimentary pigments, and their contribution to sediment color (Wolfe et al., 2006; Rein and Sirocko 2002). These studies focused on the chlorophyll *a* compound, which produces distinct color absorbances at the 650 - 700 nm wavelengths. Von Gunten et al. (2009; 2012) used this to calibrate the high resolution color scans with temperature, suggesting the utility of these compounds in future studies to produce paleo-temperature records. The presence of pheophytin *a* (a pigment and chlorophyll like molecule) in Lake El'gygytgyn was detected in very low concentrations by Leavitt et al. (personal communication) for younger samples, interestingly at the highest concentrations during the Last Glacial Maximum (LGM: 21 – 23 ka) which suggests pigment preservation variability similar to variations in TOC and measured biomarkers (Holland et al., 2013). Given the low pigment concentrations, the existence of the unique pigment color spectra reflections between the 650 to 700 nm bands (Wolfe et al., 2006; Rein and Sirocko, 2002) were not detected; however, Leavitt et al. (personal communication) did identify multiple pigment degradation compounds (Table 1), many of which may still retain a color signal. Future

work could be devoted to classifying and understanding these pigments in relationship to sediment color, as the compounds are potentially useful for paleo-lacustrine investigations.

4.5 Sediment Color and Mineralogy

Establishing the link between sediment color, lake processes and their relationship to climate change parameters allow for the use of color as a potential climate proxy. This work calibrates color, particularly the hue parameter, in the context of the chemical and physical weathering processes of the lake catchment, which can then be applied to the hue record for the entire of the sediment core.

Much like the application of biomarker investigations, additional study of the color record can also be applied to particular time intervals. MIS 31 has been identified as a "super interglacial" interval (Melles et al., 2012) with a direct correlation to warming in Antarctica. Further validation of the color proxy could involve a similar suite of analysis as presented above in chapter III; analyzing sediment samples for bulk mineralogy, clay mineralogy, and iron oxide signals could determine if the super interglacial characteristics hold for this interval.

Potential statistical investigations including time series and wavelet analyses can illustrate the sensitivity and connections of the color record to both regional and global climate shifts. Analysis of the hue record with other high resolution proxy records, can further computer modelling studies, to elucidate poorly understood orbitally forced climate mechanisms proposed by Raymo and Huybers (2008). Basic wavelet analysis of different portions of the hue color parameter (Figure 1) are suggestive of the existence of

orbital parameters such as precession, and other additional potential climate shifts occurring on shorter time scales.

Additional attention should be paid to discrepancies in data within the Lake El'gygytgyn science team, as the results from this work fail to replicate the work of past studies. Clay mineral analysis, completed by Asikainen et al. (2007), as well as more recent analysis of surface sediments by Wennrich et al. (2013) demonstrate inconsistent methods of measurement (Table 2). Corroborating the different data sets is critical as these differences could imply either drastic shifts in lake catchment processes occurred during periods of modern sedimentation, or re-analysis of past work is required. The presence/absence of certain minerals also has implications for the sediment record; for example, identification of the redox sensitive minerals siderite ($FeCO_3$) and rhodochrosite ($MnCo_3$) by Wennrich et al. (2013), and the presence of "siderite like" and "rhodochrosite like" magnetic signals from Murdock et al. (2013) could help understand redox processes within the lake. However, XRD, SEM and FTIRS analysis of the heavy mineral fractions of the sediment samples from MIS 8 through 12 from this work could not confirm the presence of these minerals, and future work could resolve the understanding of the reduction and oxidation properties of the lake water during different time intervals.

4.6 Conclusions

The ability of the Lake El'gygytgyn record to capture climate changes has been demonstrated in multiple proxies by this work. Biomarker analysis of specific organic compounds show significant differences in lake production over time. Concentrations of

these compounds not only demonstrate that the interglacials MIS 9 and 11 were significantly warmer than surround glacial intervals, but also capture the long duration of MIS 11. Sedimontological investigations conducted within the same time span, including the measurement of sediment mineralogy and color, further elucidate the nature of climate change in the Arctic region. The validation of the hue color record as a proxy for wet/dry intervals reveals MIS 9 and 11 as perhaps periods of higher precipitation in conjunction with their notable warmth. Additionally, the hue record suggests other wet time intervals, including MIS 6 and 10. Given the length of the sediment record available, future analysis will also show sensitivity to climate changes during intervals rarely captured in terrestrial records, contributing to the understanding of how climate change is expressed in our global proxy records. Future studies then have the potential to extend and contribute new knowledge of paleoclimactic changes to 3.6 ma, which is critical for sensitive regions such as the Arctic and how these regions are affected by climate change.

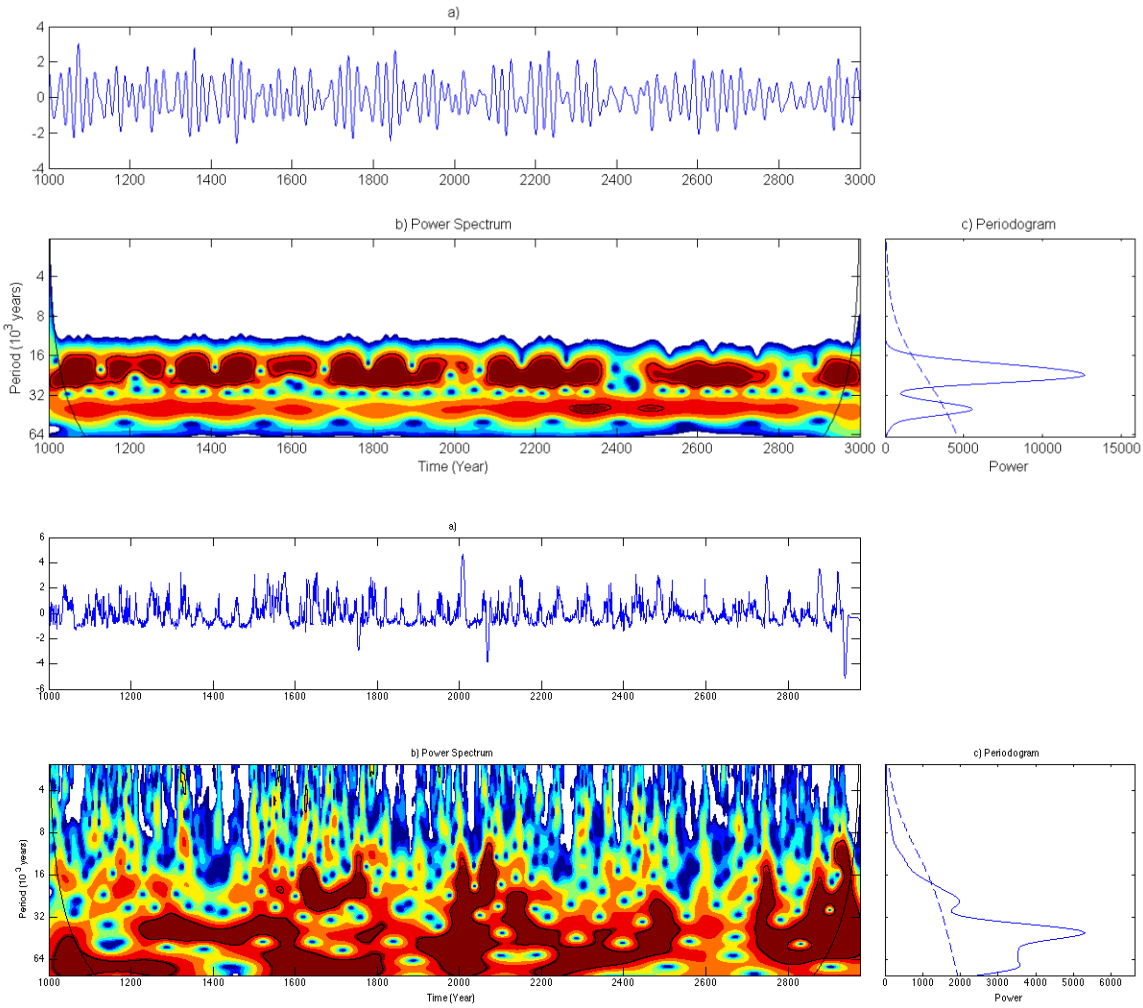

Figure 4.1: Matlab wavelet analysis (Torrence and Compo, 2013) demonstrating the precession and obliquity patterns observed for the insolation curve (top) and the hue record (bottom). For this time period ("41 kyr world") the obliquity signal is predominant; however a precessional signal is also observed.

Compound	Characterization	Source
Sed A	Derivative of scytonemin	UVr photoprotectant of cyanobacteria
Sed B	Derivative of scytonemin	UVr photoprotectant of cyanobacteria
Sed C	Derivative of scytonemin	UVr photoprotectant of cyanobacteria
Pig X	Unknown	Possible chlorophyll derivative
Chlorophyll *a*	Chlorophyll compound	Ubiquitous algal pigment
Pheo B	Derivative of Chlorophyll *B*	Green Algae
Pheo A	Derivative of Chlorophyll *a*	Ubiquitous algal pigment
B-car beta-carotene	Pigment	Ubiquitous algal pigment

Table 4.1: Table representing the compounds analyzed by Leavitt et al. (Personal communication), for a suite of Lake El'gygytgyn samples from core LZ-1029 – 6. 11 samples were analyzed, (14 cm to 214 cm depth; 4 – 31 ka). The only un-degraded pigment found was low concentrations of pheophytin at 130 and 140 cm depth (20 – 23 ka).

	Methods		Results		Reference
	This Work	**Other Work**	**This Work**	**Other Work**	
Clay Mineralogy: **Past 65 ka**	Filter mounted clay slides	"Bread and Butter" smear slides	- Clay mineral assemblages remain unchanged. - Implies physical erosion and transport of clays	- Cold periods = more chlorite - Warm periods = more smectite - Implies authigenic clay formation	Asikainen et al., 2007
Clay Mineralogy: **Modern Sediments**	XRD clay analysis Peaks identified by hand selection	XRD clay analysis Peaks identified with MacDiff software	1 to 40% total clay No Kaolinite	15 – 35 % total clay Up to 3% kaolinite	Wennrich et al., 2013
Bulk Mineral Assemblage	XRD – peaks identified by hand selection	XRD – Quax software package	No siderite No rhodochrosite No calcite No dolomite	.1 % siderite .6 % rhodochrosite 2.0 % calcite 1.5% dolomite	Wennrich et al., 2013
Fe – Oxides: **Weight Percent**	Fe Digestion (CDB method)	XRD – Co radiation	.2 to .8 % by weight iron oxides	3 to 5 % by weight iron oxides	Wennrich et al., 2013

Table 4.2: Breakdown of the discrepancies between this work, and the work conducted by previous authors on Lake El'gygytgyn sediments.

REFERENCES

Albrecht, P., Ourisson, G.: Triterpene Alcohol isolation from Oil Shale. Science, 163, 1192-1193, 1969.

Asikainen, C. A., Francus, P., Brigham-Grette, J.: Sedimentology, clay mineralogy and grain-size indicators of 65 ka of climate change from El'gygytgyn Crater Lake, Northeastern Siberia, J Paleolimnol, 37,105-122, 2007. DOI 10.1007/s10933-006-9026-5

Balsam, W. L., Beeson, J. P., Sea-floor sediment distribution in the Gulf of Mexico, Deep Sea Research, 50, 1421-1444, 2003.

Balsam, W. L., Deaton, B.C., Damuth, J. E., The effects of water content on diffuse spectrophotometry studies of deep-sea sediment cores, Marine Geology, 149, 177-189, 1998.

Bard, E., Delaygue, G., Rostek, F., Antonioli,F., Silenzi,S., Schrag, D.P., Hydrological conditions over the western Mediterranean basin during the deposition of cold Sapropel 6 (ca. 175 kyr BP), Earth Planet Sci Lett, 202, 481-494, 2002.

Barranco, F.T., Balsam,W.L., Deaton, B.C.: Quantitative reassessement of brick red lutites
— evidence from réflectance spectrophotometry. Marine Geology 89 (3–4), 299–314, 1989.

Bechtel, A., Smittenberg, R.H., Bernasconi, S.M., Schubert, C.J., Distribution of branched and isoprenoid tetraether lipids in an oligotrophic and a eutrophic Swiss lake: insights into sources and GDGT-based proxies. Org Geochem, 41, 822-832, 2010.

Belyi, V. and Belaya, B.: Late stage of the Okhotsk-Chukchi Volcanogenic Belt development (upstream of the Enmyvaam River), NEISRI FEB RAS, Magadan, Russia, 108 pp., 1998.

Belyi, V. and Raikevich, M. I.: The El'gygytgyn lake basin (geological structure, morphostructure, impactites, problems of investigation and preservation of nature), NEISRI FEB RAS, Magadan, 27 pp., 1994.

Blackburn, S.I.: Sterols of four species of dinoflagellates from the genus Prorocentrum. Phytochemistry, 52, 659-668, 1999.

Blaga, C.I., Reichart, G.-J., Schouten, S., Lotter, A.F., Werne, J.P., Kosten, S., Mazzeo, N., Lacerot, G., Sinninghe Damsté, J.S.: Branched glycerol dialkyl tetraethers in lake sediments: Can they be used as temperature and pH proxies? Org Geochem, 41, 1225-1234, 2010.

Bourbonniere, R.A., Meyers, P.A.: Sedimentary geolipid records of historical changes in the watersheds and productivities of Lakes Ontario and Erie. Limnol Oceanogr, 41, 352–359, 1997.
Bray, E. E. and Evans, E. D.: Distribution of n-paraffins as a clue to recognition of source beds, Geochim. Cosmochim. Acta, 22, 2-15, 1961.

Brigham Grette, J.: New perspectives on Beringian Quaternary paleogeography, stratigraphy, and glacial history. Quaternary Sci Rev, 20, 15-24, 2001.

Brown, B.E., and Bailey, S.W.; Chlorite Polytypism: II. Crystal Structure of a One-layer Cr-Chlorite. American Mineralogist, 28, 42-61, 1963.

Caissie, B.E.: Diatoms as recorders of Sea Ice in the Bering and Chukchi seas: Proxy development and application, PhD Dissertation, Univeristy of Massachusetts Amherst, 1-164, 2012.

Castañeda I.S., Werne J.P. and Johnson, T.C.: Influence of climate change on algal community structure and primary productivity of Lake Malawi (East Africa) from the Last Glacial Maximum to present. Limnol Oceanogr, 54, 2431-2447, 2009.

Castañeda I.S., Werne J.P., Johnson, T.C., and Powers, L.A.: Organic geochemical records from Lake Malawi (East Africa) of the last 700 years, part II: biomarker evidence for recent changes in primary productivity. Palaeogeography, Palaeoclimatology, Palaeoecology, 303, 140-154, 2011.

Castañeda, I. S., and Schouten, S.: A review of molecular organic proxies for examining modern and ancient lacustrine environments, Quaternary Sci Rev, 30, 2851-2891, 10.1016/j.quascirev.2011.07.009, 2011.

Chapligin, B., Meyer, H., Swann, G.E.A., Meyer-Jacob,C., and Hubberten,H.-W.: A 250 ka oxygen isotope record from diatoms at Lake El'gygytgyn, far east Russian Arctic. Clim Past, 2013.

Clark, R.N., Swayze, G.A., Wise, R., Livo, E., Hoefen, T., Kokaly, R., Sutley, S.J., 2007, USGS digital spectral library splib06a: U.S. Geological Survey, Digital Data Series 231.

Cranwell, P. A., Eglinton, G., Robinson, N.: Lipids of aquatic organisms as potential contributors to lacustrine sediments - II. Org Geochem, 11, 513–527, 1987.

Cranwell, P.A.: Chain length distribution of n-alkanes from lake sediments in relation to post-glacial environmental change. Freshwater Biol, 3, 259–265, 1973.

Cunningham, L., Vogel, H., Wennrich, V., Juschus, O., Nowaczyk, N., Rosen, P.: Amplified bioproductivity during Transition IV (332,000 -342,000 yr ago): evidence from the geochemical record of Lake El'gygytgyn. Clm past, 2013

D'anjou, R. M., Wei, J. H., Castañeda, I. S., Brigham-Grette, J., Petsch, S. T., Finkelstein, D. B.: High-latitude environmental change during MIS 9 & 11: Biogeochemical evidence from Lake El'gygytgyn, Far East Russia, Clim Past, 2013

Deaton, B. and Balsam, W., Visible Spectroscopy – A Rapid Method For Determining Hematite and Goethite Concentration in Geological Materials, (JOURNAL!), 1991.

Debret, M., Desmet, M., Balsam, W., Copard, Y., Francus, P., Laj, C. Spectrophotometer analysis of Holocene sediments from an anoxic fjord: Saanich Inlet, British Columbia, Canada, Marine Geology, 229, 15-28, 2006.

Debret, M., Sebag, D., Desmet, N., Balsam, W., Copard, Y., Mourier, B., Susperrigui, A.-S., Arnaud, F., Bentaleb, I., Chapron, E., Lallier-Verges, E., Winiarski, T.: Spectrocolorimetric interpretation of sedimentary dynamics: The new "Q7/4 diagram", Earth Sci Rev, 109, 1-19, 2011.

Deplazes, G., Lüchge, A., Peterson, L.C., Timmermann, A., Hamann, Y., Hughen, K. A., Röhl, U., Laj, C., Cane, M. A., Sigman, D. M., Haug, G. H.: Links between tropical rainfall and North Atlantic climate during the last glacial period. Nature Geoscience, 6, 213-217, 2013. DOI: 10.1038/NGEO1712

Didyk B. M., Simoneit B.R.T., Brassell S. C. and Eglinton G.: Organic geochemical indicators of paleoenvironmental conditions of sedimentation. Nature, 272, 216-222, 1978.

Eglinton, G., Hamilton, R.J.: Leaf epicuticular waxes. Science, 156, 1322–1335, 1967.
Epica Community Members: Eight glacial cycles from an Antarctic ice core, Nature, 429, 2004.
Epica Community Members: Eight glacial cycles from an Antarctic ice core, Nature, 429, 2004.

Fawcett, P.J., Werne, F.P., Anderson, R.S., Heikoop, J.M., Brown, E.T., Berke, M.A., Smith,
S.J., Goff, F., Donohoo-Hurley, L., Cisneros-Dozal, L.M., Schouten, S., Sinnighe Damsté, J.S, Huang, Y., Toney, J., Fressenden, J., WoldeGabriel, G., Atudorei, V., Geissman, J.W., Allen, C.D.: Extended megadroughts in the southwestern United States during Pleistocene interglacials. Nature, 470, 518-521, 2011.

Ficken, K.J., Li, B., Swain, D.L., Eglinton, G.: An n-alkane proxy for the sedimentary input of submerged/floating freshwater aquatic macrophytes. Org Geochem, 31, 745–749, 2000.
Grimalt, J., Albaiges, J.: Sources and occurrence of C12-C22 n-alkanes distributions with even carbon-number preference in sedimentary environments. Geochim. Cosmochim. Acta, 51, 1379-1384, 1987.

Hao, Q., Wang, L., Oldfield, F., Peng, S., Qin, L., Song, Y., Xu, B., Qiao, Y., Bloemendal, J., Guo, Z.: Delayed build-up of Arctic ice sheets during 400,000-year minima in insolation variability. Nature, 490, 393, 2013.

Hayes, J. B.: Polytypism of Chlorite in Sedimentary Rocks, Clays and Clay minerals, 18, 285-306, 1970.

Helmke, J.P., Shulz, M., Bauch, H. A.: Sediment Color Record from the Northeast Atlantic Reveals Patterns of Millennial-Scale Climate Variability during the past 500,000 years, Quaternary Research, 57, 49 – 57, 2002. doi:10.1006/qres.2001.2289

Holland, A., Wilkie, K.M., Petsch,S.T., Burns, S.J., Castañeda, I.S. Brigham-Grette,J., and El'gygytgyn Scientific Party: Using bulk and compound specific isotope analysis to explore connections between episodic isotope depletion and anoxia at Lake El'gygytgyn, Far East Russian Arctic. Clim Past, 2013.

Hopmans, E. C., J. W. H. Weijers, E. Schefuß, L. Herfort, J. S. Sinninghe Damste´, and S. Schouten (2004), A novel proxy for terrestrial organic matter in sediments based on branched and isoprenoidtetraether lipids, Earth Planet. Sci. Lett., 224, 107–116

Hopmans, E., Schouten, S., Pancost, R.D., van der Meer, M.T.J., Sinninghe Damsté, J.S.: Analysis of intact tetraether lipids in archaeal cell material and sediments by high performance liquid chromatography/atmospheric pressure chemical ionization mass spectrometry. Rapid Commun Mass Sp, 14, 585-589,2000.

Huston, M.M. and Brigham-Grette,J.: Paleogeographic significance of Middle Pleistocene glaciomarine deposits on Baldwin Peninsula, Northwest Alaska. Ann Glaciol, 14, 111-119, 1990.
hydrocarbons as molecular indicators of floral changes in Upper Carboniferous/Lower Permian strata of the Saar-Nahe Basin, southwest Germany. Geochim. Cosmochim. Acta, 58, 4689-4702, 1994.

Jackson, M.L.: Soil Chemical Analysis: Advanced Course. pp 44 -52, 1969. Parallel Press, Madison Wisconsin.

Jacob, J., Disnar, J.R., Boussafir, M., Sifeddine, A., Albuquerque, A.L.S., Turcq, B.: Pentacyclic triterpene methyl ethers in recent lacustrine sediments (Lagoa do Caçó, Brazil). Org. Geochem, 36, 449–46, 2005.

Ji, J., Shen, J., Balsam, W., Chen, J., Liu, L., Liu, X.: Asian monsoon oscillations in the northeastern Qinghai-Tibet Plateau since the late glacial as interpreted from visible reflectance of Qinghai Lake sediments, Earth and Plan Sci Lett 233, 61-70, 2005. doi:10.1016/j.epsl.2005.02.025

Laskar, J., Robutel, P., Joutel, F., Gastineau, M., Correia, A.C.M., and Levrard, B.: A long-term numerical solution for the insolation quantities of the Earth. Astron Astrophys, 428, 261-285, 2004.

Lawrence, K. T., Herbert, T. D., Brown, C. M., Raymo, M. E., and Haywood, A. M.: High Amplitude Variations in North Atlantic Sea Surface Temperature During the Early Pliocene Warm Period, Paleoceanography, 24, 10/1029/2008PA001669, 2010.

Layer, P. W.: Argon-40/argon-39 age of the El'gygytgyn impact event, Chukotka, Russia, Meteorit Planet Sci, 35, 591-599, 2000.

Leavitt, P., Personal Communication

Lisiecki, L. E., Raymo, M.: A Pliocene-Pleistocene stack of 57 globally distributed benthic δ18O records, Paleoceanography, 20, 10.1029/2004pa001071, 2005.

Loutre, M. F., and Berger, A.: Marine Isotope Stage 11 as an analogue for the present interglacial, Global Planet Change, 36, 209-217, 10.1016/s0921-8181(02)00186-8, 2002.

Lozhkin, A. V., Anderson, P. M. M., T.V. , and Minyuk, P. S.: The pollen record from El'gygytgyn Lake: implications for vegetation and climate histories of norther Chukotka since the late middle Pleistocene, J. Paleolimnol, 37, 135 - 153, 10.1007/s10933006-9018-5, 2007a.

Lozhkin, A.V., Anderson, P.M., Matrosova, T.V., Minyuk, P.S., Brigham-Grette,J., Melles,M.: Continuous record of environmental changes in Chukotka during the last 350 thousand years. Russian Journal of Pacific Geology, 1, No.6, 550-555, 2007b.

Lozhkin, A.V., and Anderson, P.M.; Vegetation responses to interglacial warming in the Arctic, examples from Lake El'gygytgyn, northeast Siberia. Clim Past, 2013.

Luthi, D., Le Floch, M., Bereiter, B., Blunier, T., Barnola, J.-C., Siegenthaler, U., Raynaud, D., Jouzel, J., Fischer, H., Kawamura, K., and Stocker, T.F.: High-resolution carbon dioxide concentration record 650,000 - 800,000 years before present. Nature, 453, 379-382, 2008.

Maslanik, J.A., Fowler, C., Stroeve, J., Drobot, S., Zwally, J., Yi, D., Emery, W.: A younger, thinner Arctic ice cover: Increased potenital for rapid, extensive sea-ice loss. Geophysical Research Letters, 34, L24501 – L24506, 2007.

Melles, M., Brigham-Grette, J., Glushkova, O.Y., Minyuk, P.S., Nowaczyk, N.R., Hubberton, H.-W.; Sedimentary geochemistry of core PG131 from Lake El'gygytgyn – a sensitive record of climate variability in the East Siberian Arctic during the past three glacial-interglacial cycles. J. Paleolimnol, 37, 89-104, 2007.

Melles, M., Brigham-Grette, J., Minyuk, P. S., Nowaczyk, N. R., Wennrich, V., DeConto, R. M., Anderson, P. M., Andreev, A. A., Coletti, A., Cook, T. L., Haltia-Hovi, E., Kukkonen, M., Lozhkin, A. V., Rosen, P., Tarasov, P., Vogel, H., and Wagner, B.: 2.8 Million Years of Arctic Climate Change from lake El'gygytgyn, NE Russia, Science, 2012.

Meyers P.A., Ishiwatari R.: The early diagenesis of organic matter in lacustrine sediments. In: Organic Geochemistry: Principles and Applications (eds. M.H. Engels and S.A. Macko), 185-209, 1993. Plenum Press, New York.

Meyers, P.A., and Ishiwatari, R.: 1995, Organic matter accumulation records in lake sediments: *in* Lerman, A., et al., eds., Physics and Chemistry of Lakes: New York, Springer-Verlag, p. 279-289.

Meyers, P.A.: Applications of organic geochemistry to paleolimnological reconstructions: a summary of examples from the Laurentian Great Lakes. Org Geochem, 34, 261–289, 2003.
Meyers, P.A.: Organic geochemical proxies of paleooceanographic, paleolimnologic, and paleoclimatic processes: Org Geochem, 27, 213-250, 1997.

Minyuk, P.S., Borkhodoev, V.Y., Wennrich, V.: Inorganic data from El'gygytgyn Lake sediments: stages 6 – 11, Climate of the past, 2013.

Mix, A.C., Rugh, W., Pisias, N. G., Viers, S., Leg 138 Shipboard Sedimentologists, and the Leg 138 Scientific Party: Color Reflectance Spectroscopy: A Tool for Rapid Characterization of Deep-Sea Sediments. Proceedings of the Ocean Drilling Program Initial Reports, 138, 67-77,1992.

Moore, D.M., and Reynolds, R.C. Jr.: X-Ray Diffraction and the Identification and Analysis of Clay Minerals, 2nd ed. Oxford University Press, New York, 1997.

Nolan, M., and Brigham-Grette, J.: Basic hydrology, limnology, and meteorology of modern Lake El'gygytgyn, Siberia, J. Paleolimnol, 37, 17-35, 2007.

Nolan, M: Analysis of local AWS and NCEP/NCAR reanalysis data at Lake El' gygytgyn, and its implications for maintaining multi-year lake-ice covers, Clim Past, 2013

Ortiz, J. D., Polyak, L., Grebmeier, J. M., Darby, D., Eberl, D. D., Naide, S., Nof, D.: Provenance of Holocene sediment in the Chukchi-Alaskan margin based on combined diffuse spectral reflectance and quantitative X-Ray Diffraction analyses, Glob and Plan Change, 68, 73-84, 2009.

Pearson, E. J., Juggins, S., Talbot, H. M., Weckström, J., Rosén, P., Ryves, D. B., Roberts, S. J., and Schmidt, R.: A lacustrine GDGT-temperature calibration from the Scandinavian Arctic to Antarctic: Renewed potential for the application of GDGT-paleothermometry in lakes, Geochim. Cosmochim. Acta, 75, 6225-6238, 2011.

Peterse, F., Kim, J.H., Schouten, S., Kristensen, D.K., Kos, N., Sinninghe Damsté, J.S.: Constraints on the application of the MBT/CBT palaeothermometer at high latitude environments (Svalbard, Norway). Org Geochem, 40, 692-699, 2009.

Peterse, F., van der Meer, J., Schouten, S., Weijers, W.H.J., Fierer, N., Jackson, R.B., Kim, J.H., Sinninghe Damsté, J.S.: Revised calibration of the MBT-CBT paleotemperature proxy based on branched tetraether membrane lipids in surface soils. Geochim. Cosmochim. Acta, 96, 21-229, 2012.

Post, J.E.: Manganese oxide minerals: Crystal structures and economic and environmental significance, Proc Natl Acad Sci, 96, 3447- 3454, 1999.

Poynter, J.G., Eglinton, G.: Molecular composition of three sediments from hole 717C: The Bengal Fan. In: Cochran, J.R., Stow, D.A.V., et al. (Eds.), Proceedings of the Ocean Drilling Program Scientific Results 116, 155–161, 1990.

Prokopenko, A. A., Hinnov, L. A., Williams, D. F., and Kuzmin, M. I.: Orbital forcing of continental climate during the Pleistocene: a complete astronomically tuned climatic record from Lake Baikal, SE Siberia, Quaternary Sci Rev, 25, 3431-3457, 2007.

Prokopenko, A. A., Bezrukova, E. V., Khursevich, G. K., Solotchina, E. P., Kuzmin, M. I., and Tarasov, P. E.: Climate in continental interior Asia during the longest interglacial of the past 500 000 years: the new MIS 11 record from Lake Baikal Se Siberia, Clim Past, 6, 31-48, 2010.

Rampen, S.W., Schouten, S., Wakeham, S.G., Sinninghe Damsté, J.S.: Seasonal and spatial variation in the sources and fluxes of long chain diols and mid-chain hydroxy methyl alkanoates in the Arabian Sea. Org Geochem, 38, 165– 179, 2007.

Rampen, S.W. , Schouten, S., Koning, E., Brummer, G.-J.A., Sinninghe Damste, J.S.: A 90 kyr upwelling record from the northwestern Indian Ocean using a novel long-chain diol index. Earth Planet Sc Lett, 276, 207-213, 2008.

Rampen, S.W., Abbas, B.A., Schouten, S., Sinninghe Damsté, J.S.: A comprehensive study of sterols in marine diatoms (Bacillariophyta): impli- cations for their use as tracers for diatom productivity. Limnol Oceanogr, 55, 91-105, 2010.

Rampen, S.W., Willmott, V., Kim, J.-H., Uliana, E., Mollenhauer, G., Schefuß, E., Sinninghe Damsté, J.S., Schouten, S.: Long chain 1,13- and 1,15-diols as a potential proxy for palaeotemperature reconstruction. Geochim. Cosmochim. Acta, 84, 204–216, 2012.

Raymo, M. E., and Mitrovica, J. X.: Collapse of polar ice sheets during the stage 11 interglacial, Nature, 483, 453-456, 2012.

Raymo, M. E., Lisiecki, L. E., Nisanciogliu, K. H.: Plio-Pleistocene Ice Volume, Antarctic Climate, and the Global $\delta^{18}O$ Record, Science, 313, 492-495, 2006.

Raymo, M.E., and Huybers, P.: Unlocking the mysteries of the ice ages, Nature, 451, 284-285, 2008. doi:10.1038/nature06589

Rein, B., and Sirocko, F.: In-Situ reflectance spectroscopy – analyzing techniques for high-resolution pigment logging in sediment cores. Int. J. Earth Sci, 91, 950-954, 2002. DOI 10.1007/s00531-002-0264-0

Ruan, H.D., Frost, R.L., Kloprogge, J.T., Duong, L.: Infrared spectroscopy of goethite dehydroxylation: III. FT-IR microscopy of in situd study of the thermal transformation of goethite to hematite, Spectrochimica Acta Part A, 57, 967 – 981, 2002.

Schwamborn, G., Fedorov, G., Schirrmeister, L., Meyer, H., Hubberten, H.-W.: Periglacial sediment variations controlled by lake level rise and Late Quaternary climate at El'gygytgyn Crater Lake, Arctic Siberia, Boreas, 37, 55–65, 2008.

Serreze, M.C., Holland, M.M., Stroeve, J.: Presepectives on the Arctic's Shrinking Sea-Ice Cover, Science, 315, 1533 – 1536, 2007.

Sinninghe Damsté J.S., Rijpstra W.I.C., Hopmans E.C., Weijers W.H., Foesel B.U., Overmann J., Dedysh S.N.: 13,16-dimethyl octacosanedioic acid (iso-diabolic acid), a common membrane-spanning lipid of Acidobacteria subdivisions 1 and 3. Appl. Environ. Microbiol. 77, 2011.

Sinninghe Damsté, J.S., Ossebaar, J., Abbas, B., Schouten, S., Verschuren, D.: Fluxes and distribution of tetraether lipids in an equatorial African lake: constraints on the application of the TEX 86 paleothermometer and BIT index in lacustrine settings. Geochim. Cosmochim. Acta, 73, 4232-4249, 2009.

Snyder, J.A., Cherepanova, M.V., Bryan, A.: Dynamic diatom response to changing climate 0-1.2 Ma at lake El'gygytgyn, Far East Russian Arctic. Clim Past, 2013.

Sun, Q., Chu, G., Liu, M., Xie, M., Li, S., Ling, Y., Wang, X., Shi, L., Jia, G., Lü,. H.: Distributions and temperature dependence of branched glycerol dialkyl glycerol tetraethers in recent lacustrine sediments from China and Nepal. Journ. Geophys. Res. 116, 2011.

Tierney, J.E., and Russell, J.M., Distribution of branched GDGTs in a tropical lake system: implications for the application of the MBT/CBT proxy. Org Geochem, 40(9), 1032-1036, 2009.

Tierney, J. E., Russell, J. M., Eggermont, H., Hopmans, E. C., Verschuren, D., and Sinninghe Damsté, J. S.: Environmental controls on branched tetraether lipid distributions in tropical East African lake sediments, Geochim. Cosmochim. Acta, 74, 2010.

Tierney, J.E., Schouten, S., Pithcer, A., Hopmans, E.C., Sinninghe Damsté, J.S.: Core and intact polar glycerol dialkyl glycerol tetraethers (GDGTs) in Sand Pond, Warwick, Rhode Island (USA): Insights into the origin of lacustrine GDGTs. Geochim. Cosmochim. Acta, 77, 561-81, 2012.

Tisserand, A., Malaizé, B., Jullien, E., Zaragosi,S., Charlier, K., Grousset., F., African monsoon enhancement during the penultimate glacial period (MIS 6.5 ~ 175 ka) and its atmospheric impact. Paleoceanagraphy, 24, PA 2220, 2009. DOI:10.1029/2008PA001630

Torrence, C., and Compo, G.: "Wavelet Analysis software", http://atoc.colorado.edu/research/wavelets/, accessed 2013.

Torrent, J., Schwertmann, U., Fechter, H., Alferez, F.: Quantitative relationships between soil color and hematite content. Soil Science, 136-6, 354-358, 1983.

Traschel, M., Grosjean, M., Schnyder, D., Kamenik, C., Rein, B. Scanning reflectance spectroscopy (380 – 730nm): a novel method for quantitative high resolution climate reconstructions from minerogenic lake sediments, J. Paleolim, 44, 979-994, 2010. DOI 10.1007/s10933-010-9468-7

Versteegh G. J. M., Jansen J. H. F., De Leeuw J. W., and Schneider R. R.: Mid-chain diols and keto-ols in SE Atlantic sediments: a new tool for tracing past sea surface water masses? Geochim. Cosmochim. Acta 64**,** 1879–1892, 2000.

Versteegh, G.J.M., Bosch, H.-J., de Leeuw, J.W.: Potential palaeoenvironmental Vliex M., Hagemann H. W. and Püttmann W.: Aromatized arborane/fernane information of C24 to C36 mid-chain diols, keto-ols and mid-chain hydroxy fatty acids; a critical review. Org Geochem, 27, 1-13, 1997.

Voelker, A. H. L., Rodrigues, T., Billups, K., Oppo, D., McManus, J., Stein, R., Hefter, J., and Grimalt, J. O.: Variations in mid-latitude North Atlantic surface water properties during the mid-Brunhes (MIS 9–14) and their implications for the thermohaline circulation, Clim Past, 6, 531-552, 2010.

Vogel, H. , Meyer-Jacob, C., Melles, M., Brigham-Grette, J., Andreev, A.A., Wennrich. V. , Rosén, P., in review. Detailed insight into Arctic climatic variability during MIS 11 at Lake El'gygytgyn, NE Russia. Clim Past, 2013.

Volkman, J.K., Rijpstra, W.I.C., de Leeuw, J.W., Mansour, M.P., Jackson, A.E., Volkman, J.K.: A review of sterol markers for marine and terrigenous organicmatter. Org Geochem, 9, 83-99, 1986.

Volkman, J. K., Farrington, J. W., and Gagosian, R. B.: Ma- rine and terrigenous lipids in coastal sediments form the Peru upwelling region at 15°S: sterols and triterpene alcohols. Org. Geochem, 11, 463-477, 1987.

Volkman, J.K., Barrett, S.M., Dunstan, G.A., Jeffrey, S.W.: C30-C32 alkyl diols and unsaturated alcohols in microalgae of the class Eustigmatophyceae. Org Geochem, 18, 131-138, 1992.

Volkman, J.K., Barrett, S.M., Blackburn, S.I., Mansour, M.P., Sikes, E.L., Gelin, F.: Microalgal biomarkers: a review of recent research developments. Org Geochem, 29, 1163-1179, 1998.

Volkman, J.K.: Sterols in microorganisms. Appl Microbiol Biot, 60, 495-506, 2003.
Von Gunten, L., Grosjean, M., Rein, B., Urrutia, R., Appleby, P., A quantitative high-rsolution summer temperature reconstruction based on sedimentary pigments from Laguna Aculeo, central Chile, back to AD 850. The Holocene, 19, 873, 2009. DOI: 10.1177/0959683609336573

Von Gunten, L., Grosjean, M., Kamenik, C., Fujak, M., Urrutia, R., Calibrating biogeochemical and physical climate proxies from non-varved lake sediments with meteorological data: methods and case studies, J. Paleolimnol, 47, 583-600, 2012. DOI 10.1007/s10933-012-9582-9

Walker, J. R.: Chlorite Polytype Geothermometry, Clays and Clay Minerals, 41, 260-267, 1993.

Weijers, J.W.H., Schefuß, E., Schouten, S., Sinninghe Damsté, J.S.: Coupled thermal and hydrological evolution of tropical Africa over the last deglaciation. Science, 315, 1701-1704, 2007a.

Weijers, J. W. H., Schouten, S., van den Donker, J. C., Hopmans, E. C., and Sinninghe Damsté, J. S.: Environmental controls on bacterial tetraether membrane lipid distribution in soils, Geochim. Cosmochim. Acta, 71, 703-713, 10.1016/j.gca.2006.10.003, 2007b.

Wennrich, B., Francke, A., Dehnert, A., Juschus, O., Teipe, T., Vogt, C., Brigham-Grette, J., Minyuk, P.S., Melles, M.: Modern sedimentation patterns of Lake El'gygytgyn, NE Russia, derived from surface sediment and inlet streams samples, Climate of the Past, 2013.

Withers, N. 1983. Dinoflagellate Sterols. In Scheuer, P. J. [Ed.] Marine Natural Products: Chemical and Biological Perspectives, vol. 5. Academic Press, New York, pp. 87–130. 1987. Dinoflagellate sterols. In Taylor, F. J. R. [Ed.] The Biology of Dinoflagellates, vol. 21. Blackwell Scientific, Oxford, pp. 316–59.

Wolfe, A. P., Vinebrooke, R.D., Muchelutti, N., Rivard, B., Das, B., Experimental calibration of lake-sediment spectral reflectance to chlorophyll *a* concentrations: methodology and paleolimnological validation, J. Paleolimnol, 36: 91-100, 2006. DOI 10.1007/s10933-006-0006-6

Yin, Q.Z., Berger, A.: Insolation and CO_2 contribution to the interglacial climate before and after the Mid-Bruhnes Event. Nature Geosci, 3, 243-246, 2010.

Zink, K.G., Vandergoes, M.J., Mangelsdorf, K., Dieffenbacher-Krall, A.C., Schwark, L.: Application of bacterial glycerol dialkyl glycerol tetraethers (GDGTs) to develop modern and past temperature estimates from New Zealand lakes. Org Geochem, 41, 1060-1066, 2010.